Modern Applied Science
www.ccsenet.org/journal.html
Vol. 3, No. 9
September 2009

Electrospinning Preparation of $LaFeO_3$ Nanofibers

Jinxian Wang, Xiangting Dong (Corresponding author), Zhen Qu, Guixia Liu & Wensheng Yu
School of Chemistry and Environmental Engineering
Changchun University of Science and Technology
Changchun, Jilin 130022, China
Tel: 86-431-8558-2574 E-mail: dongxiangting888@yahoo.com.cn

This work was financially supported by the Science and Technology Development Planning Project of Jilin Province (Grant Nos. 20040125, 20060504, 20070402), Key Research Project of Science and Technology of Ministry of Education of China(Grant No.207026), the Science and Technology Planning Project of Changchun City(Grant No. 2007045), the Scientific Research Planning Project of the Education Department of Jilin Province (Under grant Nos. 200224, 2005109, 2007-45) and the Scientific Research Project of Environment Protection Bureau of Jilin Province(No. 2006-24)

Abstract

Polyvinyl alcohol(PVA)/[$La(NO_3)_3$+$Fe(NO_3)_3$] composite nanofibers were fabricated by electrospinning, and polycrystalline $LaFeO_3$ nanofibers were prepared by calcination of the PVA/[$La(NO_3)_3$+$Fe(NO_3)_3$] composite nanofibers at 600ºC for 10h. The samples were characterized by using X-ray diffraction spectrometry(XRD), scanning electron microscopy(SEM), thermogravimetric-differential thermal analysis(TG-DTA), and Fourier transform infrared spectrometry(FTIR). The results show that PVA/[$La(NO_3)_3$+$Fe(NO_3)_3$] composite nanofibers are amorphous in structure, and pure phase $LaFeO_3$ nanofibers are orthorhombic with space group Pn*a. The surface of as-prepared composite nanofibers is smooth, and the diameter is ca. 180nm. The diameter of $LaFeO_3$ nanofibers is smaller than that of the relevant composite fibers. The surface of the $LaFeO_3$ nanofibers becomes coarse with the increase of calcination temperatures. The diameter of $LaFeO_3$ nanofibers is about 80nm, and the length is greater than 100μm. The mass of the sample remains constant when the temperature is above 500ºC, and the total mass loss percentage is 90%. Possible formation mechanism of $LaFeO_3$ nanofibers is preliminarily advanced.

Keywords: La, Fe, $LaFeO_3$, Nanofibers, Electrospinning

1. Introduction

The science and technology of nanostructured materials is advancing at a rapid pace (Yang, 2009, Gao, 2009, Mohapatra, 2008 & Zhang, 2007). Over the past decade, the preparation and functionalization of one-dimensional nanostructured materials has become one of the most highly energized research fields(Hu, 2008 & Kar, 2006). One-dimensional nanostructured materials, such as nanowires, nanorods, nanowhiskers and nanofibers, have stimulated great interest due to their importance in basic scientific research and potential technological applications(Huynh, 2002 & Duan, 2003). They are expected to play an important role as both interconnects and functional components in the fabrication of nanoscale electronic and optoelectronic devices. In order to obtain these materials, various preparation methods have been developed including arc discharge, laser ablation, template, precursor thermal decomposition, and other methods(Iijima, 1991, Morales, 1998, Shi, 2001 & Pan, 2001). Electrospinning technique is widely applied to prepare polymers nanofibers(Li, 2004, 1151-1170). Recently, some inorganic compounds nanofibers have been prepared by electrospinning technique using electrospun fibers of polymer/inorganic composite as the precursor (Li, 2004, Zhang, 2008 & Shao, 2004). This processing involved the following three steps: (1) Preparation of a sol with suitable inorganic precursor and proper polymer, and achieving the right rheology for electrospinning process; (2) Electrospinning of the sol to obtain fibers of polymer/inorganic precursors composite; (3) Calcinations of the composite fibers to obtain final oxide fibers. It is important; however, to control all of the above three steps in order to obtain high quality fibers with the desired final properties. $LaFeO_3$ has attracted much interest recently due to their specific electrical, and catalytic properties (Dong, 1994 & Yang, 2003). A few methods on the preparation of $LaFeO_3$

nanocrystalline materials were reported (Wang, 2006, Yang, 2005, Wang, 2006, Qi, 2003 & Yang, 2006). In this paper, $LaFeO_3$ nanofibers were fabricated by calcination of the electrospun fibers of PVA/[$La(NO_3)_3$+$Fe(NO_3)_3$] composite, and some new results were obtained.

2. Experimental

2.1 Chemicals

Polyvinyl alcohol(PVA)(Mr=80000) was bought from the Third Chemical Reagents Factory of Tianjin, and iron nitrate enneahydrate[$Fe(NO_3)_3 \cdot 9H_2O$] were purchased from Tianjin Kermel Chemical Reagents Development Center. Lanthanum nitrate hexahydrate[$La(NO_3)_3 \cdot 6H_2O$] was obtained from Tianjin Guangfu Institute of Fine Chemicals. All chemicals were analytically pure and directly used as received without further purification. Distilled water was used as solvent.

2.2 Preparation of PVA/[$La(NO_3)_3$+$Fe(NO_3)_3$] composite sol

PVA/[$La(NO_3)_3$+$Fe(NO_3)_3$] composite solution was prepared by dissolving an amount of PVA powders, $La(NO_3)_3 \cdot 6H_2O$ and $Fe(NO_3)_3 \cdot 9H_2O$ in distilled water, and stirring for 5h, then remaining motionlessly for 2h. Thus, a viscous sol of PVA/[$La(NO_3)_3$+$Fe(NO_3)_3$] composite containing 9%(wt%) PVA, 3% (wt%) metallic salts, 88%(wt%) H_2O, and the molar ratio 1:1 of La^{3+} to Fe^{3+} was obtained for electrospinning processing.

2.3 Fabrication of PVA/[$La(NO_3)_3$+$Fe(NO_3)_3$] composite nanofibers and $LaFeO_3$ nanofibers

The setup used for electrospinning was indicated in Figure 1. The above composite sol of PVA, $La(NO_3)_3$, $Fe(NO_3)_3$ and H_2O mixture was contained in a plastic syringe with a stainless steel needle on its top, and the diameter of the needle was 1mm. A copper wire connected to a DC high-voltage power supply was placed in the sol, and the sol was kept in the syringe by adjusting the angle between syringe and horizon, and the angle was kept at 15º. A grounded aluminum foil served as counter electrode and collector plate. The distance between the needle tip and the collector was fixed to 15cm. Electrospinning experiments were performed when ambient temperature was greater than 18ºC and relative air humidity was 50%-60%. A voltage of 20kV was applied to the composite sol and a sprayed dense web of fibers was collected on the aluminum foil. The collected fibers were PVA/[$La(NO_3)_3$+ $Fe(NO_3)_3$] composite nanofibers. The prepared composite nanofibers were dried initially at 70ºC for 12h under vacuum, and then calcined at a heating rate of 2ºC/min and remained for 10h at 300ºC, 600ºC and 900ºC, respectively. Thus, $LaFeO_3$ nanofibers were obtained when calcination temperature was 600ºC.

2.4 Characterization methods

XRD analysis was performed with a Y-2000 X-ray diffractometer made by Dandong Aolong Radiative Instrument Co. Ltd using Cu Kα radiation and Ni filter, the working current and voltage were 20mA and 40kV, respectively. Scans were made from 20° to 100° at the speed of 3°/min, and step was 0.02°. The morphology and size of the fibers were observed with a S-4200 scanning electron microscope made by Japanese Hitachi company. TG-DTA analysis was carried out with a SDT-2960 thermal analyzer made by American TA instrument company at a temperature-rising rate of 10ºC/min under stable air conditions. FTIR spectra of the samples were recorded on BRUKER Vertex 70 Fourier transform infrared spectrophotometer made by Germany Bruker company, and the specimen for the measurement was prepared by mixing the sample with KBr powders and then the mixture was pressed into pellets, the spectrum was acquired in a wave number range from 4000cm^{-1} to 400cm^{-1} with a resolution of 4cm^{-1}.

3. Results and discussion

3.1 XRD results

In order to investigate the lowest crystallizing temperature and the variety of phases, the PVA/[$La(NO_3)_3$+$Fe(NO_3)_3$] composite fibers and samples obtained by calcining the composite fibers at different temperatures for 10h were characterized by XRD, as indicated in Figure 2. The results showed that the PVA/[$La(NO_3)_3$+$Fe(NO_3)_3$] composite fibers were amorphous in structure, only a broad peak was located around 22º, it was the typical peak of the amorphous polymer, indicating that the composite fibers were amorphous in structure. The sample was also amorphous at 300ºC. The polycrystalline $LaFeO_3$ nanofibers with single phase were synthesized when calcination temperature was in the range of 600-900ºC, the d(spacing between crystallographic plane)values and relative intensities of $LaFeO_3$ were consistent with those of JCPDS standard card(37-1493), and the crystal structure of the prepared $LaFeO_3$ was orthorhombic system with space group Pn*a.

3.2 SEM images

In order to study the morphology and size of the as-synthesized fibers, the prepared fibers were investigated by SEM, as shown in Figure 3. As seen from Figure 3, the morphology and size of the fibers varied strongly with the increase of calcination temperatures. The surface of the PVA/[$La(NO_3)_3$+$Fe(NO_3)_3$] composite nanofibers was very smooth, and the diameter of the composite fibers was about 180nm. The diameter of the fibers was ca. 120nm at 300ºC. The surface

morphology of $LaFeO_3$ nanofibers became coarse with the increase of calcination temperatures. The diameter of the synthesized $LaFeO_3$ nanofibers was ca. 80nm at 600ºC, and their lengths were greater than 100μm. The diameters of $LaFeO_3$ nanofibers were smaller than those of the PVA/[$La(NO_3)_3$+$Fe(NO_3)_3$] composite nanofibers owing to the decomposition and evaporation of PVA and NO_3^-. Figure 4 was the distribution histograms of the diameters of samples. It was found that the diameters of the samples were in narrow size. The peak values of diameters of the PVA/[$La(NO_3)_3$+$Fe(NO_3)_3$] composite nanofibers and $LaFeO_3$ nanofibers were 180nm and 80nm, respectively. It was also found from Figure 3 that the fibers were broken at 900ºC. Therefore, $LaFeO_3$ nanofibers with good morphology should be prepared at low calcination temperature.

3.3 TG-DTA analysis

TG and DTA curves of the PVA/[$La(NO_3)_3$+$Fe(NO_3)_3$] composite fibers were indicated in Figure 5. It was noted that there were mainly three stages of weight loss. The first weight loss step (6%) was in the range of 40ºC to 102ºC accompanied by a small endothermic peak near 75.62ºC in the DTA curve caused by the loss of the surface absorbed water or the residual water molecules in the composite fibers. The second weight loss step (51.6%) was noticed between 102ºC and 253ºC accompanied by an exothermic peak near 234.68ºC in the DTA curve due to the decomposition of the nitrate and side-chain of PVA. The last weight loss was 32.4% from 253ºC to 500ºC. In the DTA curve, a big and a small exothermic peak were located at 296.03ºC and 409.65ºC. These were likely to be the oxidation combustion of the PVA main chain and further decomposition of the nitrate. And above 500ºC, the TG and DTA curves were all stable, indicating that water, organic compounds, and nitrate in the composite fibers were completely volatilized and pure $LaFeO_3$ nanofibers could be obtained above 500ºC. The total weight loss rate was 90%. This result tallied with the XRD analysis.

3.3 FTIR spectra analysis

Pure PVA, PVA/[$La(NO_3)_3$+$Fe(NO_3)_3$] composite nanofibers and $LaFeO_3$ nanofibers(obtained by calcination of the relevant composite nanofibers at 600ºC for 10h) were analyzed by FTIR, as shown in Figure 6. As seen from Figure 6, PVA(Figure 6a) and PVA/[$La(NO_3)_3$+$Fe(NO_3)_3$] composite nanofibers(Figure 6b) had the identical spectra, but absorption peaks intensity of spectrum for PVA/[$La(NO_3)_3$+$Fe(NO_3)_3$] composite nanofibers was lower than those of spectrum for pure PVA. This resulted from the lower content of PVA in the PVA/[$La(NO_3)_3$+$Fe(NO_3)_3$] composite nanofibers. All absorption peaks were attributed to PVA at 3334cm^{-1}, 2945cm^{-1}, 1704cm^{-1}, 1488cm^{-1}, 1305cm^{-1}, 1091cm^{-1}, 815cm^{-1} corresponding to the stretching vibrations of hydroxyl group(ν_{O-H}), C-H bond(ν_{C-H}), carbonyl group($\nu_{C=O}$), C-H bond(ν_{C-H}), C-C bond(ν_{C-C}), C-O bond(ν_{C-O}), and O-H bond(ν_{O-H}), respectively. It was seen from Figure 6c that all peaks of PVA disappeared, and at low wave number range, a new absorption peak at 567cm^{-1} appeared. The new absorption peak was ascribed to the vibration of metal-oxygen bond, indicating that $LaFeO_3$ was formed. The results of FTIR analysis were in good agreement with XRD results.

3.4 Possible formation mechanism of $LaFeO_3$ nanofibers

Possible formation mechanism of $LaFeO_3$ nanofibers was indicated in Figure 7. $La(NO_3)_3 \cdot 6H_2O$, $Fe(NO_3)_3 \cdot 9H_2O$ and PVA were mixed with distilled water to form sol with certain viscosity. PVA acted as template during the formation processing of $LaFeO_3$ nanofibers. La^{3+}, Fe^{3+} and NO_3^- were mixed with or absorbed onto PVA molecules to fabricate PVA/[$La(NO_3)_3$+$Fe(NO_3)_3$] composite fibers under electrospinning. During calcination treatment of the composite fibers, solvent water would remove to the surface of the PVP/[$La(NO_3)_3$+$Fe(NO_3)_3$] composite fibers and eventually evaporated from the composite fibers. With the increasing in calcination temperature, PVA molecular chains were broken, PVA and NO_3^- would oxidize and volatilize gradually, La^{3+} and Fe^{3+} were oxidized into $LaFeO_3$ crystallites in air, and many crystallites were sintered to form small $LaFeO_3$ nanoparticles, these small nanoparticles were combined into big particles, and these particles were mutually connected to generate $LaFeO_3$ nanofibers.

4. Conclusions

4.1 PVA/[$La(NO_3)_3$+$Fe(NO_3)_3$] composite nanofibers were fabricated by electrospinning. Polycrystalline $LaFeO_3$ nanofibers were synthesized by calcining the relevant composite fibers at 600ºC.

4.2 TG-DTA analysis showed that the mass of the PVA/[$La(NO_3)_3$+$Fe(NO_3)_3$] composite fibers remained constant when the temperature was above 500ºC, and the total mass loss percentage was 90%.

4.3 XRD analysis revealed that the composite fibers were amorphous in structure. The crystal structure of $LaFeO_3$ nanofibres was orthorhombic system with space group Pn*a.

4.4 SEM images indicated that the surface of the prepared composite fibres was smooth, and the diameter of the composite nanofibres was about 180nm. The diameters of $LaFeO_3$ nanofibers were smaller than those of the composite nanofibers. The surface of the $LaFeO_3$ nanofibers became coarse with the increase of calcination temperatures. The diameter of $LaFeO_3$ nanofibers was ca. 80nm, and their lengths were greater than 100μm.

References

Dong, X. T., Guo, Y. Z., Yu, D. C., et al. (1994). Study of synthesis and electrical properties of $LaFeO_3$ ultrafine powders. *Mater. Sci. & Technol.*, 2(1), 11-14.

Duan, X. F., Huang, Y., Agarwal, R., Lieber, C. M. (2003). Single-nanowire electrically driven lasers. *Nature*, 421, 241-245.

Gao, X. B., Dong X. T., Fan L. J. et al. (2009). Fabrication and Characterization of Nd^{3+}:YAG Nanofibers. *Chinese Journal of Lasers*, 36(6): 1517-1522.

Hu, X. K., Qian, Y. T., Song, Z. T., et al. (2008). Comparative study on MoO_3 and H_xMoO_3 nanobelts: structure and electric transport. *J. Chem Mater,* 20(4), 1527-1533.

Huynh, W. U., Dittmer, J. J., Alivisatos, A. P. (2002). Hybrid nanorod-polymer solar cells. *Science*, 295, 2425-2427.

Iijima, S. (1991). Helical microtubules of graphitic carbon. *Nature*, 354, 56-58.

Kar, S., Chaudhuri, S. (2006). Shape selective growth of CdS one-dimensional nano-structures by a thermal evaporation process. *J. Phys. Chem. B*, 110(10), 4542-4547.

Li, D., Xia, Y. N. (2004). Direct fabrication of composite and ceramic hollow nanofibers by electrospinning. *Nano Lett.*, 4(5), 933-938.

Li, D., Xia, Y. N. (2004). Electrospinning of Nanofibers: Reinventing the Wheel. *Adv. Mater.*, 16(14), 1151-1170.

Mohapatra, S. K., Misra, M., Mahajan, V. K., et al. (2008). Synthesis of Y-branched TiO_2 nanotubes. *Materials Letters*, 62, 1772-1774.

Morales, A. M., Lieber, C. M.(1998). A laser ablation method for the synthesis of crystalline semiconductor nanowires. *Science*, 279, 208-211.

Pan, Z. W., Dai, Z. R., Wang. E.L. (2001). Nanobelts of semiconducting oxides. *Science*, 291, 1947-1949.

Qi, X. W., Zhou, J., Yue, Z. X., et al. (2003). A simple way to prepare nanosized $LaFeO_3$ powders at room temperature. *Ceramic International*, 29(3), 347-349.

Shao, C. L., Guan, H. Y., Liu, Y. C., et al. (2004). A novel method for making ZrO_2 nanofibres via an electrospinning technique. *J. Crystal Growth*, 267, 380-384.

Shi, W. S., Zheng, Y. F., Wang, N., et al. (2001). A general synthetic route to III-V compound semiconductor nanowires. *Adv. Mater.*, 13, 591-594.

Wang, D., Chu, X. F., Gong, M. L. (2006). Single-crystalline $LaFeO_3$ nanotubes with rough walls: synthesis and gas-sensing properties. *Nanotechnology*, 17, 5501-5505.

Wang, Y. P., Zhu, J. W., Zhang, L. L., et al. (2006). Preparation and characterization of perovskite $LaFeO_3$ nanocrystals. *Mater. Lett.*, 60, 1767-1770.

Yang, Q. H., Fu, X. X. (2003). Analysis of photocatalytic oxidation activity of nano-$LaMO_3$(M=Cr, Mn, Fe, Co) compounds. *J. Chin. Ceram. Soc.*, 31(3), 254-256.

Yang, X. F., Dong, X. T. Wang, J. X., et al. (2009). Glycine-assisted hydrothermal synthesis of YPO_4:Eu^{3+} nanobundles. *Materials Letters*, 63, 629-631.

Yang, Z., Huang, Y., Dong B., et al. (2006). Controlled synthesis of highly ordered $LaFeO_3$ nanowires using a citrate-based sol-gel route. *Mater. Res. Bull.*, 41(2), 274-281.

Yang, Z., Huang, Y., Dong, B., et al. (2005). Fabrication and structural properties of $LaFeO_3$ nanowires by an ethanol-ammonia-based sol-gel template route. *Applied physics A, Materials science & processing*, 81(3), 453-457.

Zhang, S. H., Dong, X. T., Xu, S. Z., et al. (2007). Preparation and characterization of TiO_2@SiO_2 submicron-scaled coaxial cables via a static electricity spinning technique. *Acta Chimica Sinica*, 65(23), 2675-2679.

Zhang, S. H., Dong, X. T., Xu, S. Z., et al. (2008). Preparation and characterization of TiO_2/SiO_2 composite hollow nanofibers via an electrospinning technique. *Acta Materiae Compositae Sinica*, 25(3), 138-143.

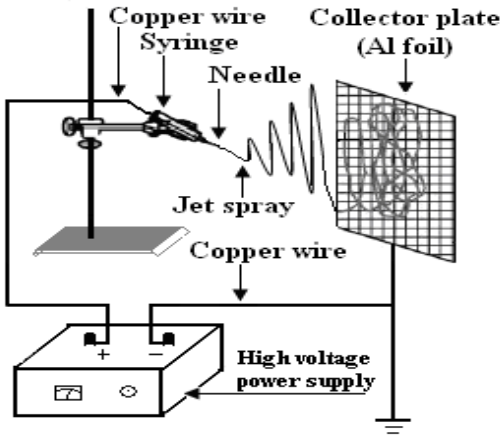

Figure 1. Schematic diagram of electrospinning setup

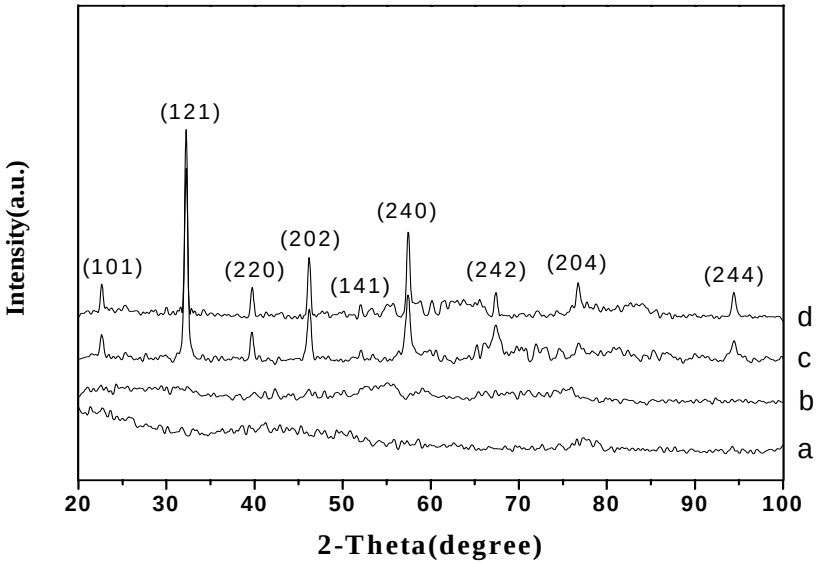

Figure 2. XRD patterns of samples

a. PVA/[$La(NO_3)_3$+$Fe(NO_3)_3$] composite fibers b. 300ºC c. 600ºC d. 900ºC

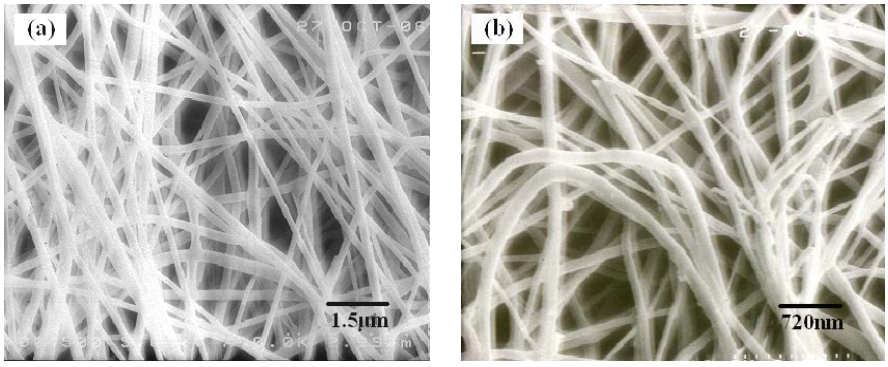

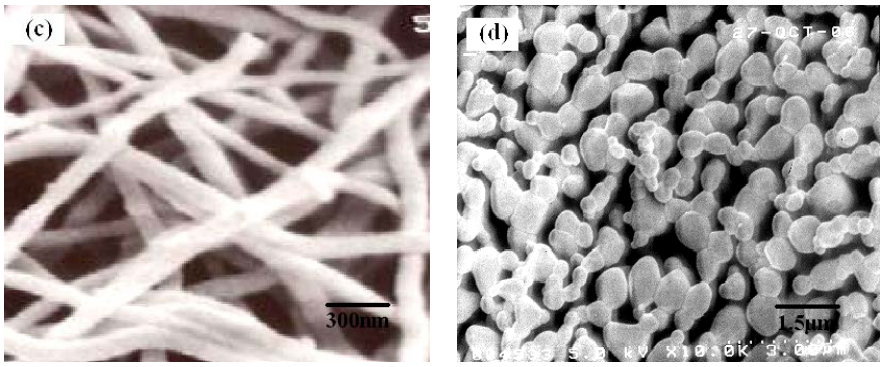

Figure 3. SEM images of the fibers obtained at different temperatures
(a) PVA/[$La(NO_3)_3$+$Fe(NO_3)_3$] composite fibers (b) 300ºC (c) 600ºC (d) 900ºC

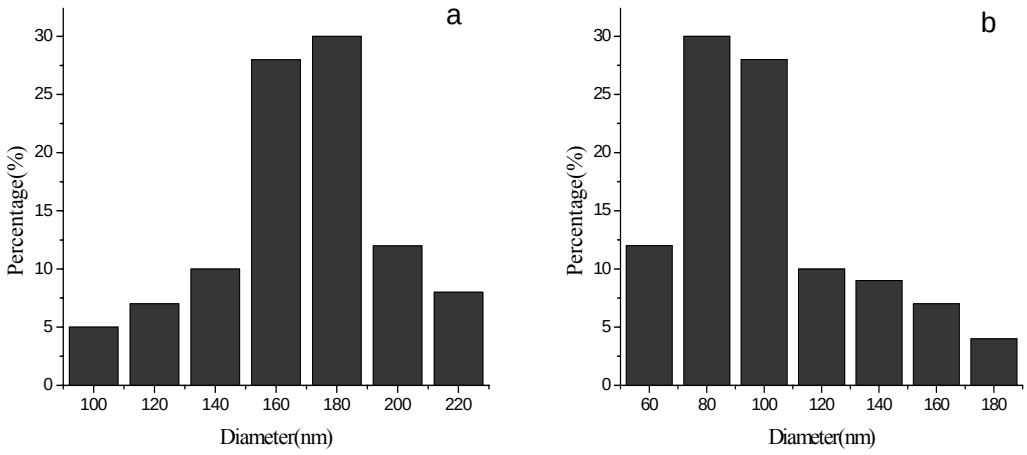

Figure 4. Distribution histograms of the diameters of samples
a. PVA/[$La(NO_3)_3$+$Fe(NO_3)_3$] composite fibers b. 600ºC

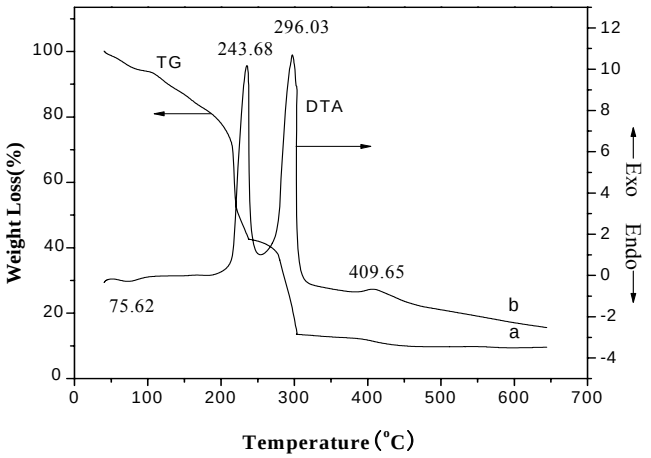

Figure 5. TG-DTA curves of PVA/[$La(NO_3)_3$+$Fe(NO_3)_3$] composite fibers

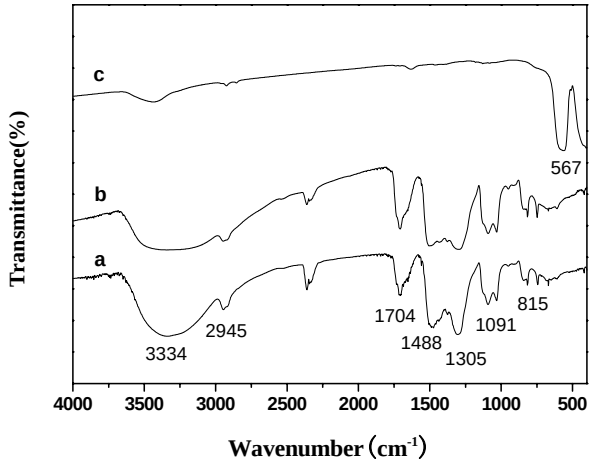

Figure 6. FTIR spectra of the samples

a. Pure PVA b. PVA/[$La(NO_3)_3$+$Fe(NO_3)_3$] composite fibers c. $LaFeO_3$ nanofibers

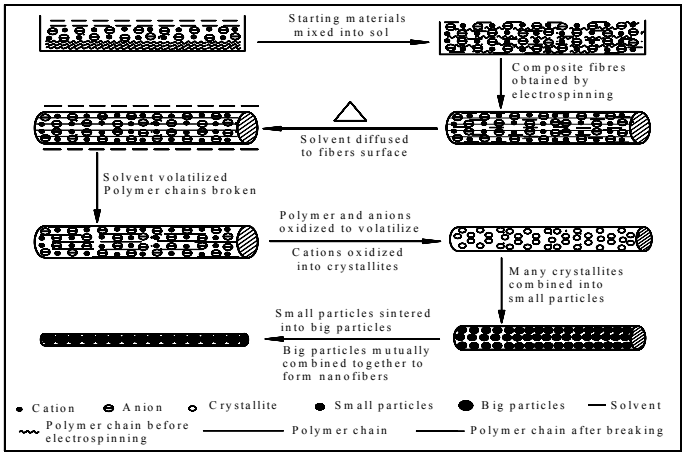

Figure 7. Illustrative diagram of possible formation mechanism of $LaFeO_3$ nanofibers

Modern Applied Science
www.ccsenet.org/journal.html
Vol. 3, No. 9
September 2009

A New Method of Hierarchical Text Clustering Based on Lsa-Hgsom

Jianfeng Wang, Lina Ma, Xinye Li, Yangxiu Zhou & Dong Qiao
Technology College, North China Electric Power University
No 282, Rei Xiang Street, Baoding, China
Tel: 86-312-752-3461 E-mail: wjf611@yahoo.com.cn

This research was supported by Young Teachers Research Foundation of North China Electric Power University No.93222805

Abstract

Text clustering has been recognized as an important component in data mining. Self-Organizing Map (SOM) based models have been found to have certain advantages for clustering sizeable text data. However, current existing approaches lack in providing an adaptive hierarchical structure within in a single model. This paper presents a new method of hierarchical text clustering based on combination of latent semantic analysis (LSA) and hierarchical GSOM, which is called LSA-HGSOM method. The text clustering result using traditional methods can not show hierarchical structure. However, the hierarchical structure is very important in text clustering. The LSA-HGSOM method can automatically achieve hierarchical text clustering, and establishes vector space model (VSM) of term weight by using the theory of LSA, then semantic relation is included in the vector space model. Both theory analysis and experimental results confirm that LSA-HGSOM method decreases the number of vector, and enhances the efficiency and precision of text clustering.

Keywords: Text Clustering, Hierarchical GSOM, Latent Semantic Analysis, Vector Space Model

1. Introduction

With the popularization and application of Internet network has become an important part of the people's working and living, and various search engines have been an indispensable tool to retrieve the necessary resources for the people. However, the Internet search engine can often find thousands of search results. Even if some useful information is obtained, it is often mixed with a lot of "noises" to waste the users' time and money. Therefore, in order to efficiently and economically retrieve the resource subset relevant to the given search request and with the appropriate number, the Text clustering is performed and becomes one of important and hot research fields in data mining (R.D.Lawrence,1999,pp.171-195).

Text clustering is different from Text classification. The latter has them for each category while Text clustering has no category annotates in advance. The Text clustering is to divide the Text sets into several clusters according to the Text contents, and requires the similarity of the Text contents in the clusters as great as possible and that of different clusters as small as possible. It can organize the Web Text effectively, but also form a classification template to guide the classification of the Web Text. Therefore, the Text clustering is an important content in the domain of data mining, and also acts as a very important role in text mining. The general procedure of the text clustering methods is as follows. Firstly, the documents to be clustered are transformed into some sets of terms, and term weights are assigned to each term of the sets, then some term weights constitute a feature vector that represents a text. In fact, text clustering means text contents clustering. However, the term sets can not concern with the text contents in clustering process. Therefore, a way of improving text clustering effect is that clustering of documents is based on text conception (or semantic content). The existing methods of text clustering can obtain a single clustering structure; however, the result can not show hierarchical relation among categories. In fact, people need to understand the hierarchical relation among categories. In order to overcome this defect, we present a new method of hierarchical text clustering called LSA-HGSOM method. The method applies the theory of LSA to construct a VSM (Vector Space Model), and achieves text clustering through conception statistic computation. Therefore, the method advances the speed and precision of text clustering. Moreover, the clustering method can achieve automatically hierarchical text clustering through a hierarchical GSOM method (called HGSOM).

2. The theory of LSA

2.1 Term Matrix

LSA (Latent Semantic Analysis) (S.T.Dumais,1988,pp.281-285) is one of the most popular linear document indexing methods which produce low dimensional representations using word co-occurrence which could be regarded as semantic relationship between terms. LSA aims to find the best subspace approximation to the original document space in the sense of minimizing the global reconstruction error (the Euclidean distance between the original matrix and its approximation matrix). It is fundamentally based on SVD (Singular Value Decomposition) and projects the document vectors into the subspace so that cosine similarity can accurately represent semantic similarity. Given a term-document matrix $X=[x_1,x_2,\cdots,x_n]\in R^m$ and suppose the rank of X is r, LSA decomposes X using SVD as follows:

$$X=U\sum V^T \tag{1}$$

where $\sum=diag(\sigma_1,\cdots\sigma_r)$ and $\sigma_1\geq\sigma_2\geq\cdots\geq\sigma_r$ are the singular values of X. $U=[u_1,\cdots,u_r]$ and u_i is called the left singular vector. $V=[v_1,\cdots,v_r]$ and v_i is called the right singular vector. LSA uses the first k vectors in U as the transformation matrix to embed the original documents into a k-dimensional space.

2.2 Singular Value Decomposition

After the matrix X is established, we can acquire an approximate matrix X_k of the matrix X with k orders, where $k<\min(m,n)$. By the singular value decomposition (G. W. Furnas, 1988, pp.36-40), a matrix X can be denoted as a product of three matrices.

$$X=U\sum V^T \tag{2}$$

In formula (2), U and $\sum$ denote the left and the right singular vector matrices of the matrix X respectively; the diagonal matrix $\sum$ consists of singular values of the matrix X according to the arrangement with descending order. We select the foremost k maximal singular values of the matrix X, and establish an approximate matrix X_k with k order.

$$X_k=U_k\sum_k V_k^T \tag{3}$$

In formula (3), U_k and V_k are orthogonal vectors. X_k denotes approximately the term vector matrix X, the row vectors of U_k represent the term vectors, and the row vectors of V_k represent the document vectors. After using singular value decomposition and selecting approximate matrices of k orders, the model of LSA acquires some good effects as follows. For one thing, the disadvantageous factors in original term matrix are decreased. Moreover, the semantic relation between terms and documents becomes more obvious. In addition, the dimension of VSM is decreased greatly, and so the speed of clustering is advanced. In short, through the process of LSA, the VSM of documents has the following merits.

The dimension of VSM is decreased greatly, and so the speed of clustering is advanced.

3. The theory of GSOM

3.1 The Self-Organizing Map (SOM)

SOM is an unsupervised neural network model that maps high-dimensional input space to low-dimensional output space. When the resulting map is a two-dimensional topology, the intuitive visualization provides good exploration possibilities. The drawback of this approach is the pre-fixed structure of the output space and lack of providing hierarchical relations between the input spaces. (A. Rauber, 1999, pp. 302-311)

3.2 The Growing Self Organizing Map (GSOM)

The GSOM algorithm is composed of three phases, initialization, growing and smoothing. Soon after the smoothing phase, the generated map can be queried and the input data vectors clustered (A. Hsu, 2003, pp. 2131-2140).

3.2.1 Initialization phase:

Initialize the weight vectors of the starting nodes (usually four) with random numbers between 0 and 1.

Calculate the growth threshold (GT) for the given data set of dimension D according to the spread factor (SF) using the formula $GT=-D\times\ln(SF)$

3.2.2 Growing Phase:

a) Present input to the network.

b) Determine the weight vector that is closest to the input vector mapped to the current feature map (winner), using Euclidean distance. This step can be summarized as: find q' such that $\left|v-w_{q'}\right|\leq\left|v-w_q\right|\forall q\in N$ where v, w are the

inputs and weight vectors respectively, q is the position vector for nodes and N is the set of natural numbers.

c) The weight vector adaptation is applied only to the neighborhood of the winner and the winner itself. The neighborhood is a set of neurons around the winner, but in the GSOM the starting neighborhood selected for weight adaptation is smaller compared to the SOM (localized weight adaptation). The amount of adaptation (learning rate) is also reduced exponentially over the iterations. Even within the neighborhood, weights that are closer to the winner are adapted more than those further away. The weight adaptation can be described by

$$w_j(k+1)=\begin{cases} w_j(k) & if\ j \notin N_{k+1} \\ w_j(k)+LR(k)\times(x_k-w_j(k)) & if\ j \notin N_{k+1} \end{cases} \tag{4}$$

Where the Learning Rate $LR(k)$, $k \in N$ is a sequence of positive parameters converging to zero as $k \to \infty$. $w_j(k)$, $w_j(k+1)$ are the weight vectors of the node j before and after the adaptation and N_{k+1} is the neighborhood of the winning neuron at the $(k+1)th$ iteration. The decreasing value of $LR(k)$ in the GSOM depends on the number of nodes existing in the map at time k.

d) Increase the error value of the winner (error value is the difference between the input vector and the weight vectors).

e) When $TE_i \geq GT$ (where TE_i is the total error of node i and GT is the growth threshold). Grow nodes if i is a boundary node. Distribute weights to neighbors if i is a non-boundary node.

f) Initialize the new node weight vectors to match the neighboring node weights.

g) Initialize the learning rate (LR) to its starting value.

h) Repeat steps 2 – 7 until all inputs have been presented and node growth is reduced to a minimum level.

3.2.3 Smoothing phase.

a) Reduce learning rate and fix a small starting neighborhood.

b) Find winner and adapt the weights of the winner and neighbors in the same way as in growing phase.

The growth threshold is based on the number of dimensions of the dataset and the spread factor (SF). SF is a predetermined value in the range 0-1, with zero allowing least spread and one, maximum spread. A limited spread with a smaller SF value should ideally be the starting map. Once significant clusters are identified, they can be used as the basis for further analysis with a higher SF value.

4. Text clustering method based on LSA--HGSOM

4.1 Conception of Text Clustering

Text clustering is the process of assigning the documents in a document base to different categories, and is a typical machine learning problem with no supervising. A species is some groups of documents. Documents within one species are more similar than those among different species. Therefore, the aim of text clustering is to group the documents: minimizing the similarity among different species and maximizing the similarity within a species.

Clustering analysis is the process that assigns similar documents to the same categories through computing the degree of similarity among all documents. By the singular value decomposition, the row vectors of v k are the vectors of texts. Therefore, we apply the row vectors of VK to calculating the degree of similarity among documents. The degree of similarity is generally denoted by cosine distance, which is defined as follows:

$$Sim(i,j)=\frac{\sum_{m=1}^{k} W_{im}\times W_{jm}}{\sqrt{\sum_{m=1}^{k}(W_{im})^2\times\sum_{m=1}^{k}(W_{jm})^2}} \tag{5}$$

Where $Sim(i,j)$ is the degree of similarity between text i and j ; where W_{im}, and W_{jm} denote the values of the rows i and j of the column m in the matrix Vk respectively.

4.2 Dimensionality Reduction

Reduction of the data dimensionality may lead to significant savings of computer resources and processing time. However the selection of fewer dimensions may cause a significant loss of the document local neighborhood information. Due to this compromise, we have chosen to use the popular and well studied singular value decomposition.

SVD is used to rewrite an arbitrary rectangular matrix, such as a Markov matrix, as a product of three other matrices: $X=U\sum V^T$. As a Markov matrix is symmetric, both left and right singular vectors (U and V) provide a mapping from the document space to a newly generated abstract vector space. The elements $(\lambda_0,\lambda_1,\cdots,\lambda_{r-1})$ of the diagonal matrix S, the singular values, appear in a magnitude decreasing order. One of the more important theorems of

SVD states that a matrix formed from the first n singular triplets $\{U_i, \lambda_i, V_i\}$ of the SVD (left vector, singular value, right vector combination) is the best approximation to the original matrix that uses n degrees of freedom. The technique of approximating a data set with another one having fewer degrees of freedom, known as dimensional reduction, works well, because the leading singular triplets capture the strongest, most meaningful, regularities of the data. The latter triplets represent less important, possibly spurious, patterns. Ignoring them actually improves analysis, though there is the danger that by keeping too few degrees of freedom, or dimensions of the abstract vector space, some of the important patterns will be lost.

After reducing the dimension, documents are represented as n-dimensional vectors in the diffusion space, and can be clustered by using HGSOM.

4.3 HGSOM Clustering

Hierarchical clustering techniques are categorized into agglomerative (bottom-up) and divisive (top-down) approaches (A.Hsu,2003,pp.2131-2140). Agglomerative clustering starts with one point clusters and recursively merges two or more similar clusters until all the clusters are encapsulated into one final cluster. Divisive clustering considers the entire dataset as one cluster and then recursively splits the most appropriate cluster until a stopping criterion is achieved. For details on clustering algorithms refer to. The hierarchical clustering model presented in this section builds a hierarchy of clusters in a novel manner. It does not follow a traditional bottom-up or top-down approach, but using GSOM as the basis and utilizing its spread factor. Since the spread factor takes the value between 0 and 1, to avoid missing any significant sub groupings, a set of values across the whole range (0-1) are initialized.

The GSOM uses a threshold value, GT, to decide when to initiate new node growth (Amarasiri,2000,pp.601-614). GT will decide the amount of spread of the feature map to be generated. Therefore, if only an abstract picture of the data is required, a large GT will result in a map with a fewer number of nodes (A.Hsu,2003,pp.2131-2140). Similarly, a smaller GT will result in the map spreading out more. Node growth in the GSOM is initiated when the error value of a node exceeds the GT. The total error value for node i is calculated as:

$$TE_i = \sum_{H_i} \sum_{j=1}^{D} (x_{i,j} - w_j)^2 \tag{6}$$

where H_i is the number of hits to the node i and D is the dimension of the data. $X_{i,j}$ and w_j are the input and weight vectors of the node i, respectively. For a boundary node to grow a new node, it is required that

$$TE_i \geq GT \tag{7}$$

The GT value has to be experimentally decided depending on the requirement for the map growth. As can be seen from (7), the dimension of the data set will make a significant impact on the accumulated error (TE) value, and as such will have to be considered when deciding the GT for a given application. Since $X_{i,j} \geq 0$, $W_j \leq 1$, the maximum contribution to the error value by one attribute (dimension) of an input would be,

$$\max \left| x_{i,j} - w_j \right| = 1 \tag{8}$$

Therefore, from (7)

$$TE_{\max} = D \times H_{\max} \tag{9}$$

where $TE_{\max}$ is the maximum error value and is the maximum possible number of hits. If H_t is considered to be the number of hits at time (iteration) t, the GT will have to be set such that

$$0 \leq GT < D \times H(t) \tag{10}$$

Therefore, GT has to be defined based on the requirement of the map spread. It can be seen from (10) that the GT value will depend on the dimensionality of the data set as well as the number of hits. Thus, it becomes necessary to identify a different GT value for data sets with different dimensionality. This becomes a difficult task, especially in applications such as data mining, since it is necessary to analyze data with different dimensionality as well as the same data under different attribute sets. It also becomes difficult to compare maps of several datasets since the GT cannot be compared over different datasets. Therefore, the user definable parameter is introduced. The SF can be used to control and calculate the GT for GSOM, without the data analyst having to worry about the different dimensions. The growth threshold is defined as

$$GT = D \times f(SF) \tag{11}$$

where $SF \in R, 0 \leq SF \leq 1$, and $f(SF)$ is a function of SF, which is identified as follows.

The total error TE_i of a node i will take the values

$$0 \le TE_i \le TE_{\max} \tag{12}$$

where $TE_{\max}$ is the maximum error value that can be accumulated. This can be written as

$$0 \le \sum_{H} \sum_{j=1}^{D} (x_{i,j} - w_j)^2 \le \sum_{H_{\max}} \sum_{j=1}^{D} (x_{i,j} - w_j)^2 \tag{13}$$

Since the purpose of the GT is to let the map grow new nodes by providing a threshold for the error value, and the minimum error value is zero, it can be argued that for growth of new nodes,

$$0 \le GT \le \sum_{H_{\max}} \sum_{j=1}^{D} (x_{i,j} - w_j)^2 \tag{14}$$

Since the maximum number of hits $(H_{\max})$ can theoretically be infinite, (14) becomes $0 \le GT \le \infty$. According to the definition of spread factor, it is necessary to identify a function $f(SF)$ such that $0 \le D \times f(SF) \le \infty$

A function that takes the values $0 \to \infty$, when x takes the values 0 to one, is to be identified. A Napier logarithmic function of the type $y = -a \times \ln(1-x)$ is one such equation that satisfies these requirements. If $\mu = 1 - SF$ and

$$GT = -D \times \ln(1-\eta) \tag{15}$$

then

$$GT = -D \times \ln(SF) \tag{16}$$

Therefore, instead of having to provide a GT, which would take different values for different data sets, the data analyst can now provide a value - SF, which will be used by the system to calculate the GT value depending on the dimensions of the data. This will allow HGSOM to be identified with their spread factors and can form a basis for comparison of different maps.

During cluster analysis, it may be necessary (and useful) for the analyst to study the effect of removing some of the attributes (dimensions) on the existing cluster structure. This might be useful in confirming opinions on non-contributing attributes on the clusters. The spread factor facilitates such further analysis since it is independent of the dimensionality of the data. This is very important, as the growth threshold depends on the dimensionality.

5. Experiments

We applied the theory of LSA method to construct the VSM, and applied the HGSOM network to achieve text clustering. We collected 500 documents to carry on the text clustering. These documents were classified into three large-scale species and six child species: Education (Includes campus (CAM) and high school education (HSE)), Economics (Includes industrial (IND) and agriculture (AGR) economics), and Medicine (Includes clinic (CLI) and nurse (NUR)). After the feature selection, we obtained 1863 feature words.

5.1 Experiment 1

We applied directly the words matrix D to carry on the text clustering, and the number of input node was 1863. In this case we could not acquire satisfactory result using HGSOM. The training speed of the network is very slow, and the result of text clustering is not correct. We think that the wrong result comes of too many input nodes. So we could not acquire good result using HGSOM network.

5.2 Experiment 2

In view of the result of the experiment 1, we choose k=785 through the process of LSA. After that, the number of input nodes is reduced to 785. We applied the HGSOM clustering algorithm to the documents clustering. The speed of training is improved greatly, and the results of clustering are shown in the table 1and table 2. We applied average accuracy (AA%) (Jiang Ning,2002,pp.5) to evaluate the results of text clustering.

In view of the result of the experiment 1, we choose k=785 through the process of LSA. After that, the number of input nodes is reduced to 785. We applied the HGSOM clustering algorithm to the documents clustering. The speed of training is improved greatly, and the results of clustering are shown in the table 1and table 2. We applied average accuracy (AA%) (Jiang Ning,2002,pp.5) to evaluate the results of text clustering.

In table 1 and table 2, the clustering results are satisfactory; therefore, HGSOM method is feasible for hierarchical text clustering. From table 1 and table 2, we can see that the results of table 1 are better than the results of table 2.The reason of acquiring this result is that the documents have more similar feature words among sub-layers than those documents among large-scale species, which impacts on the result of text clustering.

6. Conclusions

We can draw the conclusions from above experiments as follows:

(1) The present LSA-HGSOM method is feasible for text clustering.

(2) LSA-HGSOM method can achieve automatically hierarchical text clustering, and overcome the shortcomings of traditional methods.

(3) LSA-HGSOM network is limited for text clustering. If there are many input nodes, we can not acquire good result.

(4) LSA-HGSOM method can enhances the efficiency and precision of text clustering.

In this paper, we proposed a new text clustering method LSA-HGSOM. In this method, it firstly makes preprocess of texts, and introduced LSA theory to improve the precision of clustering and reduce the dimension of feature vector. Then it used HGSOM to execute the clustering to the texts, In the experiment, the result shows that LSA-HGSOM method would get a better effect in the text clustering.

References

A.Hsu, S.L.Tang & S.K.Halgamuge. (2003). An unsupervised hierarchical dynamic self-organising approach to cancer class discovery and marker gene identification in microarray data, *Bioinformatics,* vol.19, pp.2131-2140.

A.Rauber & D.Merkl. (1999). Using self-organizing maps to organize document archives and to charakterize subject matter: How to make a map tell the news of the world, *In DEXA'99: Proceedings of the 10th International Conference on Database and Expert Systems Applications. London, UK: Springer-Verlag,* pp.302-311.

Amarasiri, R., & Alahakoon, D. (2000). *Applying Dynamic Self Organizing Maps for Identifying Changes in Data Sequences. IEEE Transactions on Neural Networks, Special Issue on Knowledge Discovery and Data Mining,* 11(3).pp.601-614.

G.W.Furnas. (1988). Information retrieval using a singular-value-decomposition model of latent semantic structure. *[c] In Proceedings of SIGIR'88,* 1988, pp.36-40.

Jiang Ning & Shi Zhong-zhi. (2002). Bayesian posteriori model selection for text clustering, *Journal of computer research and development,* pp.5.

R. D. Lawrence, G.S.Almasi & H.E.Rushmeier. (1999). A scalable parallel algorithm for selforganizing maps with applications to sparsedata mining problems, *Data Mining and Knowledge Discovery*, 3,171-195.

S.T.Dumais. (1988). Using latent semantic analysis to improve information retrieval. *In CHI'88 Proceedings*. 281-285.

Table 1. The clustering result of the first layer by HGSOM method

	Medicine	Education	Economics
(AA)%	88.5	90.2	86.3

Table 2. The clustering result of the sub-layer by HGSOM method

	CLI	NUR	CAM	HSE	IND	AGR
(AA)%	79.6	79.1	84.1	82.9	85.4	84.9

Modern Applied Science
www.ccsenet.org/journal.html
Vol. 3, No. 9
September 2009

Design of the License Plate Recognition Platform Based on the DSP Embedded System

Zhikun Zhang & Qilan Huang
School of Electrical Engineering & Automatic, Tianjin Polytechnic University, Tianjin 300160, China

Abstract

The license plate recognition system (LPRS) is a very important development direction of the intelligent transportation systems (ITS). With the development of the society and the enhancement of human living level, the amount of vehicle increases continually and the traffic status is deteriorating gradually, which brings large pressures for the society and the environment. The increasingly crowded city traffic needs more advanced and effective traffic management and control. It has been an important research direction to utilize the license plate recognition technology to enhance the management level and the traffic efficiency, and implement safe intelligent transportation management. In this article, the design, implementation and optimization of the DSP license plate recognition system which takes the TMS320C6201 of TI Corporation as the core chip were introduced. In this system, the video frequency (VF) decoding chip first translates the analog TV image signals obtained from CCD into the digital image signals which are inputted into DSP through FIFO buffer by the control of CPLD, and then aiming at the image, DSP performs the license plate positioning, the license plate character segmentation, the license plate character identification, the optical aberrance emendation, the nonlinear emendation of speed error and other algorithm operations to obtain the result of the license plate identification.

Keywords: License plate recognition, TMS320C6201, CPLD, CCS

1. Research meanings and actuality of the license plate recognition system

In recent years, the license plate recognition system in China has entered into the stage of application, but because of the influences of many numerous factors such as the particularity and the technology in Chinese license plate, the using effect of the license plate automatic recognition system is not satisfactory, so the license plate recognition technology needs to be further enhanced. There are few products which can ensure that the recognition rate exceeds 95% and the recognition time is less than 0.5s. On the other hand, most current products are based on the application program of PC, so there costs are generally high.

Table 1 shows some data of the license plate recognition system used in China at present.

ITS is a kind of modernized traffic management system which can perform real-time monitoring to the road traffic flow information, supervise and perfect the traffic status in time, implement various real-time traffic controls rapidly and duly according to the dynamic change of the traffic flow, lighten the crowded degree of the road, reduce the running delay of the traffic vehicles and the probability of traffic accident, ensure the safety and high efficiency of the traffic, enhance the using rate and the security of the system resources, and reasonably utilize relative traffic establishments. With the development of the traffic industry, ITS is gradually emphasized by various countries and governments, and it has been widely applied in the collection and statistics of traffic information, the communication among vehicles, the management of park and the non-parking charge. The roads and the parks gradually develop to the directions such as informationization, intelligentization and self-service management, which requires higher intelligent degree for the instruments, especially for the charge roads parks, the self-service management should be extended. So it is very important to establish exact license plate recognition for confirming the vehicle identity and establishing corresponding database management system. In recent years, many countries begin to try out the non-parking charge system and the park self-service management system which mainly adopt the wireless communication measure, but for so many vehicles which have not installed the communication instruments, the costs are very high, in addition, the phenomena that the wireless cards don't accord with the vehicle information often happen. To solve these problems, some countries used the vidicon to record the images and adopted the manual observation to recognize the vehicles, which made the self-service management system to need large numbers of manual assistant works instead. To enhance the work

efficiency and recognize the vehicle information real time, the license plate recognition technology becomes an important research domain in ITS, and its tasks are to analyze and process the incepted vehicle images to automatically recognize the license plate of the auto. With the development and perfection of a series of relative technology such as the PC technology, the communication technology and the network technology, the license plate recognition system will certainly be turned from the research stage to the application and extension stage, which is very meaningful to enhance the management level and the automatization degree of the traffic system.

As the core function of the ITS, the license plate recognition system has gradually applied in the real living as its practicability is enhanced. Some license plate recognition systems occurred in the market have good recognition effect in appointed conditions and environment, but once the conditions and environment change, for example, in the environment such as fog day, rain day and night, the recognition rates of these systems will decrease rapidly even the recognitions will be rejected, and the currency of the systems will become very bad. Therefore, it is very necessary and important to find a license plate recognition method which can adapt to most environments and is more universal.

In a word, the license plate recognition technology is the necessary technology in future traffic domain, and by the drive of strongly social demands, the relative researches about the license plate recognition will emerge quickly. Based on this background, this task is proposed in the article, and the license plate recognition system studied in the task is the core and key technology in ITS, and the research possesses quite largely theoretical and practical meanings.

2. Structure and function of the license plate recognition system

In the image processing system, the TMS320C6201 DSP in TIC6x series is adopted as the processor of the system. In this system, the video frequency (VF) decoding chip first translates the analog TV image signals obtained from CCD into the digital image signals which are inputted into DSP through FIFO buffer by the control of CPLD, and then aiming at the image, DSP performs the license plate positioning, the license plate character segmentation, the license plate character identification, the optical aberrance emendation, the nonlinear emendation of speed error and other algorithm operations to obtain the result of the license plate identification. The system structure is seen in Figure 1.

2.1 Module of image acquisition

The image acquisition module of the system is mainly composed by the CCD camera, video frequency decoding chip SAA7111A, FIFO, and the sampling controller composed by CPLD. The current CCD camera outputs composite TV signals CVBS with the NTSC mode, and then SAA7111A decodes the analog TV signals to the digital video frequency signals according with ITU-RBT.601 standard, and store the data to the special video frequency FIFO chip by the control of CPLD. SAA7111A possesses six inputs of analog TV signal, and can accept CVBS or S-VIDEO signals, and automatically test and recognize the automatic switch of PAL and NTSC TV signals, and support YUV4:2:2, YUV4:1:1, YUV4:2:0, YUV4:1:0, RG and other digital video frequency outputs, and integrate anti-aliasing filtering waves, and pectination filtering parts. And the model can set up the synchronic field signals IGPV, the synchronic row signals IGPH, the effective image data output signals IDQ, the time output signals ICLK and other state signals, which can convenient for the interior interfaces and possess powerful functions.

2.2 Module of video frequency buffer, FIFO

The digital video frequency data acquisition speed of SAA7111A and the exterior data bus work speed of C6201 are different, so the FIFO is used between both to make the speed matching (seen in Figure 2). AL422B synchronic FIFO of the Averlogic Company is adopted in the article, and its maximum storage is 384K×8bits, and it supports CCIR, NTSC, PAL and other video frequency modes, and the writes and reads with different speeds. Two parallel connected FIFOs can compose the interface with 16bits which can completely accept the maximum data capacity after a frame of digitized TV image under the protocol of CCIR.601.

Because FIFO can not be seamlessly connected with the video frequency decoders SAA7111A and C6201DSP, so the exterior logic should be added to realize the mutual connection between FIFO and two decoders. The core to realize the mutual connection logic is a CPLD apparatus of EPM240F100C4.

2.3 Module of DSP processing

In 1997, American TI Company issued new generation DSP chip, TMSC6000 series, and the chip is mainly applied in multimedia, and it includes the fixed point series and the floating point series, and the fixed point series is TMS320C62xx, and the floating point series is TMS320C67xx, and both are compatible.

There are 8 parallel processing units in C6000DSP, and they are divided into two same groups. The system structure of DSP adopts very long instruction word structure (VLIW), and the single instruction word length is 32bits, and one instruction bag includes 8 instructions, and the total word length is 8×32=256bits. The wall of the chip sets up special instruction distribution module which can distribute each 256btis instruction to 8 processing unites at the same time, so multiple instructions can be performed in single cycle. When 8 processing units in the interior of the chip run simultaneously, their maximum processing capacity can achieve 6000MIPS (million instructions per second).

Because C6201DSP has only 64KB program memorizer, and the 64KB data memorizer can not fulfill the application, so the exterior memorizer must be extended. C6XDSP has EMIF bus which can be connected with various exterior equipments in the chip and out of the chip. In the article, IS42S16400SDRAM is selected as the exterior extended data memorizer, and the capacity of IS42S16400 is 4Mx16bits, and the combinations of two chips can compose an exterior memorizer with 4Mx23bits, and because the EMIF bus has the SDRAM controller, so DSP and SDRAM can be connected directly, without the glue logic.

When DSP runs off-line, it needs the exterior program memorizer to store the program codes, and when it runs on-line, the program can be loaded to run in the running space. The ST29LE010Flash with 128Kx8bit adopted in this article is the extended exterior program memorizer, and ST29LE010 belongs to the asynchrony apparatus, and it must be connected with the asynchrony memorizer of the C6201EMIF bus, and the connection of the exterior memorize and DSP is seen in Figure 3.

2.4 Module of PCI bus interface

To realize the interface between DSP of C5000 series and C6000 series with PCI bus, TI Company specially designed the PCI2040 chip which decode the output data of DSPHPI and output the data to the PCI bus, so the seamless connection between PCI bus and DSP can be realized, and the logic structure is seen in Figure 4. Through the HPI interface of PCI2040, the computer can interview the exterior memorizer of DSP, and store the frame image processed by DSP into the computer real time to display and make further processing analysis.

To realize the normal communication of DSP and computer, the drive of PCI2040 is the key. In Windows, there are three types of drive model, i.e. VxS, KMD and WDM. WDM is mainly pushed by Microsoft, and it possesses the features such as hierarchy structure and trans-platform, and it is compatible for the operation systems above Windows 98, so it is the mainstream development program model at present.

3. Introduction of the development environment

Generally speaking, the efficiency of C code is limited, but good development environment can enhance the efficiency and development speed of the code. Therefore, in 1999, TI Company pushed a kind of high-efficiency DSP integrated development environment CCS (Code Composer Studio).

CCS is the integrated development environment pushed by TI Company, and it can be used to develop the application program of DSP chip of TI. Not only the generation efficiency of objective code is high, but the transfer is convenient and the development cycle can be shortened largely.

The development environment used in the system is CCS2.2, and it integrates following tools in an opening plug-in structure.

(1) CCS integrates the code generation tools in its interior (C compiler, compilation optimizer, assembler and connecter);

(2) Software simulator;

(3) Real-time operation system DSP/BIOS;

(4) Real-time data exchange software RTDX;

(5) Real-time analysis and data visualization software, which can offer a perfect software development environment for developers.

DSP/BIOS is a simple embedded operation system, and it can largely help users to compile multi-task application programs and strengthen the supervision to the code execution efficiency.

4. Flow of software design

In the license plate recognition system, the flow of DSP can be described as follows. After the system receives the interrupt of hardware, it starts the image acquisition task to obtain the image data, transmits the image data from CPLD to the SDRAM out of DSP by EDMA, and after the image transmission ends, the system performs the quality evaluation, and the images will experience three operations such as the license plate positioning, the license plate segmentation and the character recognition. Finally, the result of the character recognition is transmitted to CPLD and the system performs the UART transmission. So the whole system can be divided into five tasks generally (seen in Table 2).

The transfers of tasks are simple, and the mode of flag signal SEM communication is mainly adopted. The transfers among tasks are seen in Figure 5.

5. Conclusions

The license plate recognition system is one important part of ITS, and comparing with past manual statistics and recognition, both the efficiency and the quality have been enhanced obviously. With the increase of vehicle amount and

the increasingly heavy load of the traffic system, only the manpower can not fulfill the real-time demands of the system, so it is the necessary result of the social development to realize the intelligent management of vehicle information. Combining with the high-speed numerical operation ability of DSP and the advantage that PC is good at the affair management and can offer good human-computer interface, the license plate recognition system can ensure high performance of the system and possess good flexibility, because the recognition is separated with the management, and the management software only needs receive the recognition result transmitted by the recognition module. The small improvement to the management software can flexibly update the license plate recognition algorithm, which can overcome the problem that in the traditional software recognition mode, because of the implementation of the recognition core in the management software, any change and improvement to the recognition core must transfer and check the whole management software.

References

Gao, Yinghui, Hou, Zhongxia & Ma, Yannan. (2007). Numeral Video Signal Processing System Based on FPGA+DSP. *Journal of Shenyang Institute of Aeronautical Engineering.* No.24(6). P.69-71.

Jiang, Simin & Liu, Chang. (2005). *Tutorial of TMS320C6000 DSP Application & Development.* Beijing: Mechanism Industry Press.

Li, Handong, Sun, Xing & Chen, Xuan. (2006). Design and Implementation of Machine Vision System Based on DSP. *Journal of Guilin University of Technology.* No.26(1). P.119-121.

Peng, Qizcong. (2004). *DSP Integration Development Environment: Principles and Application of CCS and DSP/BIOS.* Beijing: Electronic Industry Press.

Texas Instruments. (2004). TMS320C6000 DSP Enhanced Direct Memory Access (EDMA) Controller Reference Guide.

Texas Instruments. (2003). TMS320C6000 DSP Host Port Interface (HPI) Reference Guide.

Texas Instruments. (2006). TMS320C6000 DSP Inter-Integrated Circuit (I2C) Module Reference Guide.

Table 1. Some data about the current license plate recognition systems used in China

Name of corporation	Recognition rate of license plate	Recognition time
Shanghai GOLDWAY ITS Co., Ltd	>90%	0.5s-1s
Leading Process Vision	>90%	<0.3s
Beijing Hanwang Science and Technology Co., Ltd	>90%	<0.5s
Shenyang Judi	95%	<0.5s
Fred Science and Technology	>90%	<0.2s

Table 2. Division of tasks

Task	Function	PRI
LPEvaluation Task	Evaluation of image quality	2
LPOrientation Task	Positioning of license plate	2
LPSsegmentation Task	Segmentation of license plate	2
LPRecognition Task	Character recgonition	2
LPStorage Task	Storage of recognition result	1

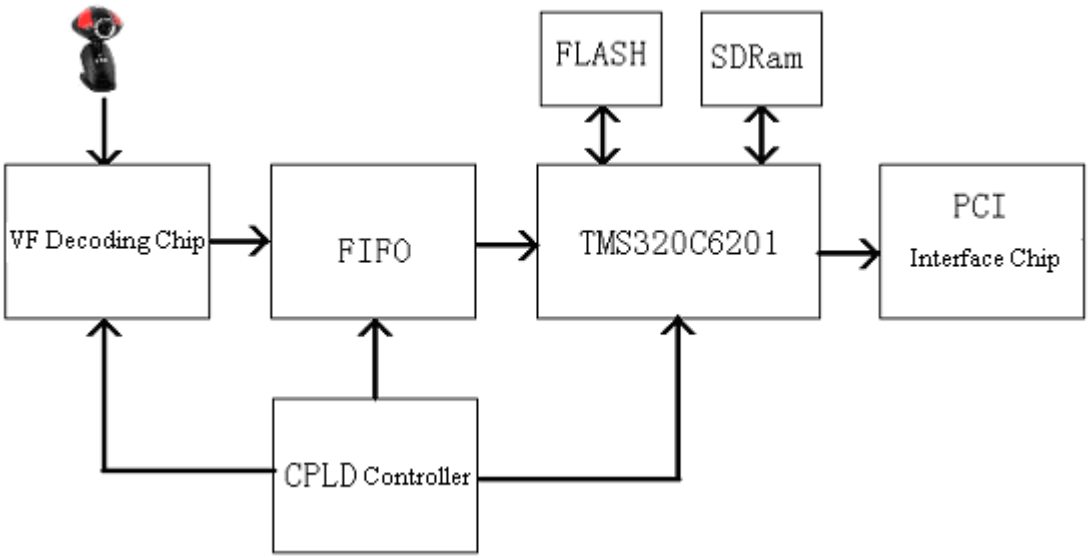

Figure 1. Structure of the License Plate Recognition System

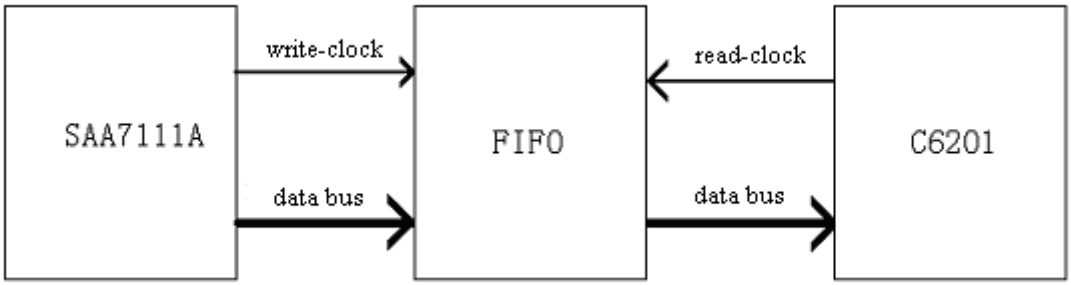

Figure 2. FIFO Buffer Interface

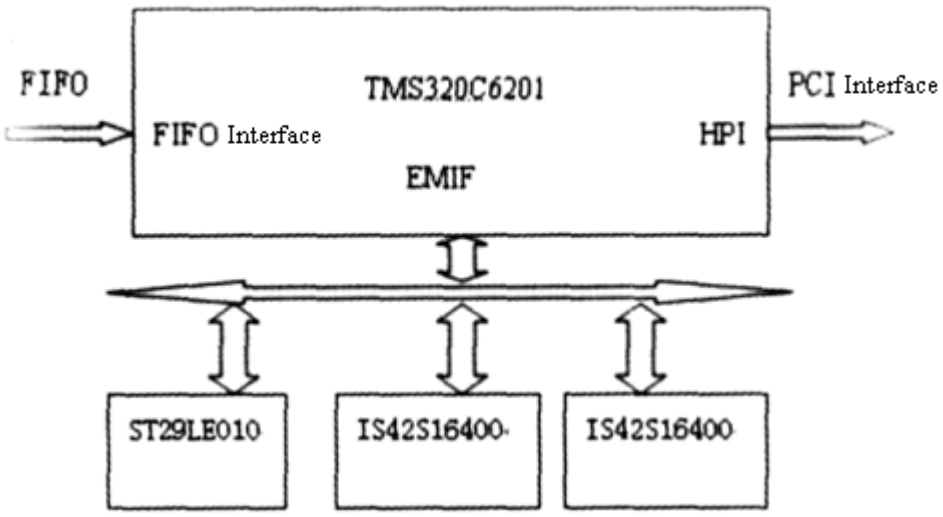

Figure 3. Extension of DSP Exterior Memorizer

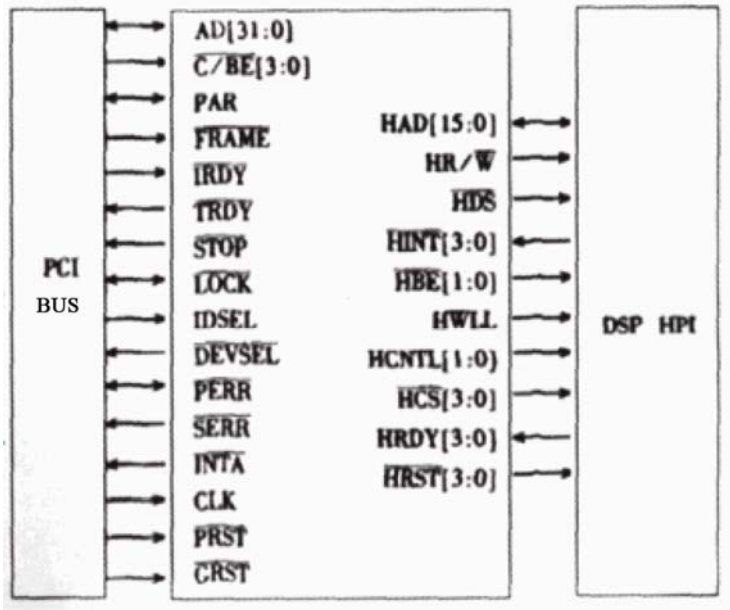

Figure 4. Applying PCI2040 to Realize PCI Interface

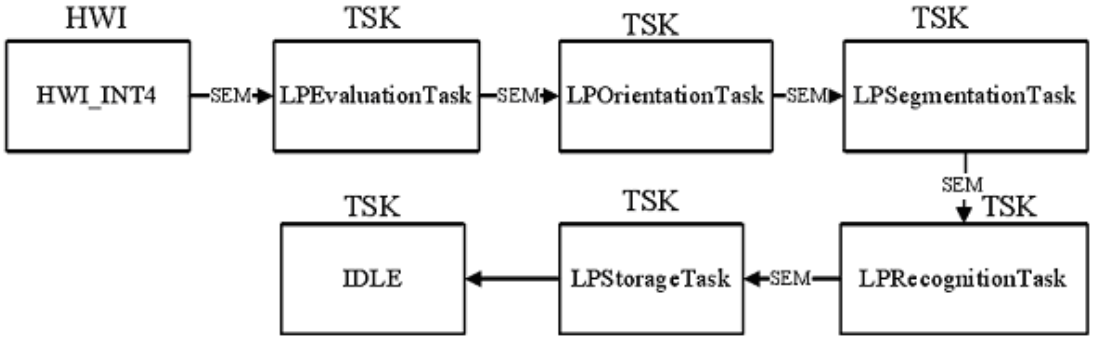

Figure 5. Transfers among Tasks

Modern Applied Science
www.ccsenet.org/journal.html
Vol. 3, No. 9
September 2009

Optimal Programming Models for Portfolio Selection with Uncertain Chance Constraint

Limei Yan
Department of Mathematics, Dezhou University
Dezhou 253023, China
E-mail: yanlimei9898@163.com

Abstract

The paper is concerned with the portfolio selection problem about how to assign one's money in security market in order to obtain the maximal profit. One type expected maximization programming model with chance constraint in which the security returns are uncertain variables are proposed in accordance with uncertainty theory. Since the provided models can not be solved by the traditional methods, the crisp equivalents of the corresponding models are discussed when the uncertain returns are chosen as some special cases such as linear uncertain variables, trapezoidal uncertain variables and normal uncertain variables. Two numerical examples with different types of uncertain variables are given in order to demonstrate the effectiveness and feasibility of the proposed programming models. Finally, the paper gives the conclusion.

Keywords: Chance constrain, Portfolio selection, Uncertain variable, Crisp equivalent programming

1. Introduction

Portfolio selection is concerned with an investor who is trying to allocate one's wealth among alternative securities so that the investment goal can be achieved. The problem was initialized by Markowitz (1952, p.77) and his mean-variance methodology has been regarded as the basis for the theory of modern portfolio selection. The pioneer work of Markowitz combined probability and optimization theory to model the investment behavior under uncertainty. An investor should always strike a balance between maximizing the return and minimizing risk for a predetermined return level. More importantly, Markowitz initially quantified investment return as the expected value of returns of securities and risk as variance from the expected value.

After Markowitz's work, scholars have been showing great enthusiasm in portfolio selection and tried to use different approaches to develop the theory of portfolio selection. Generally speaking, there are three models to deal with the portfolio selection problems with uncertain return rates. The first is expected value model (EVM), which optimizes the expected objective function subject to some expected constraints. The second chance-constrained programming (CCP) was proposed by Charnes and Cooper (1965, p.73) and developed by many scholars as means of dealing with uncertainty by specifying a confidence level at which the uncertain constraints hold. The employment and development of chance-constrained programming in portfolio selection with stochastic parameters can be found by Brockett (1992, p. 385), by Li (1995, p. 577) and by Williams (1997, p.77). Following the idea of stochastic chance-constrained programming, Liu (2002) developed a spectrum of general forms of fuzzy chance-constrained programming and a general of uncertain chance-constrained programming (2009). To use the theory of chance-constrained programming, the author tries to do something in portfolio selection problems when the return rates are assumed to be uncertain variable which is also proposed by Liu (2009). Two type of portfolio selection models are provided with uncertain return rates and the crisp equivalent programming of the corresponding models are given when the return rates are chosen as some special cases.

The rest of the paper is organized as follows. After recalling some definitions and results about uncertain measure and uncertain variable in section 2, two types of programming models for portfolio selection with chance constrain are introduced in section 3. Then section 4 discusses the crisp equivalents when the return rates are chosen as some special uncertain variables such as linear uncertain variable, trapezoidal uncertain variable and normal uncertain variable. In section 5, we provide two numerical examples to demonstrate the potential application and the effectiveness of the new

models. Finally, we conclude the paper in section 6.

2. Preliminaries

Let Γ be a nonempty set, and let A be a σ-algebra over Γ. Each element $\Lambda \in \mathrm{A}$ is called an event. In order to provide an axiomatic definition of uncertain measure, it is necessary to assign to each event Λ a number $M\{\Lambda\}$ which indicates the level that Λ will occur. In order to ensure that the number $M\{\Lambda\}$ has certain mathematical properties, Liu (2009) proposed the following five axioms:

Axiom 1 (Normality) $M(\Gamma) = 1$;

Axiom 2 (Monotonicity) $M(\Lambda_1) \le M(\Lambda_2)$ whenever $\Lambda_1 \subseteq \Lambda_2$;

Axiom 3 (Self-duality) $M(\Lambda) + M(\Lambda^{\mathrm{c}}) = 1$ for every event Λ;

Axiom 4 (Countable subadditivity) For every countable sequence of events $\{\Lambda_i\}$, we have

$M(\bigcup_{i=1}^{\infty} \Lambda_i) \le \sum_{i=1}^{\infty} M(\Lambda_i)$.

The following is the definition of uncertain measure.

Definition 1 (Liu (2009)). The set function is called an uncertain measure if it satisfies the normality, monotonicity, self-duality and countable subadditivity axioms.

Example 1 Let $\Gamma = \{\gamma_1, \gamma_2\}$. For this case, there are only 4events. Define

$M\{\gamma_1\} = 0.4,\ M\{\gamma_2\} = 0.6,\quad M(\phi) = 0,\ M(\Gamma) = 1$,

then M is an uncertain measure because it satisfies the four axioms.

Definition 2 (Liu (2009)). Let Γ be a nonempty set, A a σ-algebra over Γ, and M an uncertain measure. Then the triplet (Γ, A, M) is called an uncertain space.

The product uncertain measure is defined as follows.

Axiom 5 (Liu (2009)). (Product Measure Axiom) Let Γ_k be nonempty sets on which M_k are uncertain measures, $k = 1, 2, \cdots, n$, respectively. Then the product uncertain measure on Γ is

$$M\{\Lambda\} = \begin{cases} \sup\limits_{\Lambda_1 \times \Lambda_2 \times \cdots \times \Lambda_n \subset \Lambda} \min\limits_{1 \le k \le n} M_k\{\Lambda_k\}, & \text{if } \sup\limits_{\Lambda_1 \times \Lambda_2 \times \cdots \times \Lambda_n \subset \Lambda} \min\limits_{1 \le k \le n} M_k\{\Lambda_k\} > 0.5, \\ 1 - \sup\limits_{\Lambda_1 \times \Lambda_2 \times \cdots \times \Lambda_n \subset \Lambda^c} \min\limits_{1 \le k \le n} M_k\{\Lambda_k\}, & \text{if } \sup\limits_{\Lambda_1 \times \Lambda_2 \times \cdots \times \Lambda_n \subset \Lambda^c} \min\limits_{1 \le k \le n} M_k\{\Lambda_k\} > 0.5. \end{cases}$$

For each event $\Lambda \in \mathrm{A}$, denoted by $M = M_1 \wedge M_2 \wedge \cdots \wedge M_n$.

Definition 3 (Liu (2009)). An uncertain variable is a measurable function ξ from an uncertainty space $(\Gamma, \mathrm{A}, \mathrm{M})$ to the set of real numbers, i.e., for any Borel set B of real numbers, the set

$\{\xi \in \mathrm{B}\} = \{\gamma \in \Gamma \mid \xi(\gamma) \in \mathrm{B}\}$

is an event.

A random variable can be characterized by a probability density function and a fuzzy variable may be described by a membership function, uncertain variable can be characterized by identification function.

Definition 4 (Liu (2009)). An uncertain variable ξ is said to have a first identification function λ if

(1) $\lambda(x)$ is a nonnegative function on R such that

$\sup\limits_{x \ne y} \lambda(x) + \lambda(y) = 1;$

(2) For any set B of real numbers, we have

$$M\{\xi \in \mathrm{B}\} = \begin{cases} \sup\limits_{x \in \mathrm{B}} \lambda(x), & \text{if } \sup\limits_{x \in \mathrm{B}} \lambda(x) < 0.5, \\ 1 - \sup\limits_{x \in \mathrm{B}^C} \lambda(x), & \text{if } \sup\limits_{x \in \mathrm{B}^C} \lambda(x) \ge 0.5. \end{cases}$$

Definition 5 (Liu (2009)). The uncertainty distribution $\Phi: R \to [0,1]$ of an uncertain variable ξ is defined by

$\Phi(x) = M\{\xi \le x\}$.

3. Uncertain programming models for portfolio selection

In Markowitz models, security returns were regarded as random variables. As discussed in introduction, there does exist situations that security returns may be uncertain variable parameters. In this situation, we can use uncertain variables to describe the security returns.

Let x_i denote the investment proportion in the ith security, ξ_i represents uncertain return of the ith security, $i = 1, 2, \cdots, n$, respectively, and a the minimum return level that the investor can tolerate. Following chance constraint idea, if we want to maximize the expected value or minimize risk of the total return subject to some chance constraints, to express it in mathematical formula, the models are as follows:

$$\begin{aligned} &\max\ E[x_1\xi_1 + x_2\xi_2 + \cdots + x_n\xi_n] \\ &\text{Subject to:} \\ &M[x_1\xi_1 + x_2\xi_2 + \cdots + x_n\xi_n \le a] \le \alpha, \\ &x_1 + x_2 + \cdots + x_n = 1, \\ &x_i \ge 0,\ i = 1, 2, \cdots, n. \end{aligned} \tag{1}$$

where $\alpha \in (0,1)$ is a specified confidence level the investor given, and a is the minimum return that the investor can accept satisfying $M\{x_1\xi_1 + x_2\xi_2 + \cdots + x_n\xi_n \le a\} \le \alpha$ in which $x_1\xi_1 + x_2\xi_2 + \cdots + x_n\xi_n \le a$ means the investment risk. E is the expected value of uncertain variable. It is obvious that the combination of securities that can maximize $E[x_1\xi_1 + x_2\xi_2 + \cdots + x_n\xi_n]$ is the optimal portfolio the investor should select.

If the investor wants to minimize the investment risk with some chance constraints, then we have the following model,

$$\begin{aligned} &\min\ V[x_1\xi_1 + x_2\xi_2 + \cdots + x_n\xi_n] \\ &\text{Subject to:} \\ &M[x_1\xi_1 + x_2\xi_2 + \cdots + x_n\xi_n \ge a] \ge \alpha, \\ &x_1 + x_2 + \cdots + x_n = 1, \\ &x_i \ge 0,\ i = 1, 2, \cdots, n. \end{aligned} \tag{2}$$

where V denotes the variance of the total return which represents the risk of the investment.

4. Crisp equivalents

In general, to solve the uncertain programming model the traditional solution methods require conversion of the objective function and the chance constraints to their respective deterministic equivalents. And this process is usually hard to perform and only successful for some special cases. In the next content, we will consider several special forms of uncertain return rate ξ_i, and convert the models (1) and (2) into their crisp equivalents.

4.1 Models for linear uncertain variable

An uncertain variable ξ is called linear if it has a linear uncertainty distribution

$$\Phi(x) = \begin{cases} 0, & \text{if } x < a \\ (x-a)/(b-a), & \text{if } a \le x \le b \\ 1. & \text{if } x > b \end{cases}$$

denoted by $L(a,b)$ where a and b are real number with $a < b$.

Suppose that the return rate ξ_i of the ith security is linear uncertain variable $\xi_i = L(a_i, b_i)$ with $a_i < b_i, i = 1, 2, \cdots, n$, then

$$x_1\xi_1 + x_2\xi_2 + \cdots + x_n\xi_n = L(\textstyle\sum_{i=1}^{n} x_i a_i, \sum_{i=1}^{n} x_i b_i).$$

In accordance with the propositions of linear uncertain variables, the expected value and variance of the total return are as follows,

$$E[x_1\xi_1 + x_2\xi_2 + \cdots + x_n\xi_n] = \frac{1}{2}\textstyle\sum_{i=1}^{n} x_i(a_i + b_i),$$

$$V[x_1\xi_1 + x_2\xi_2 + \cdots + x_n\xi_n] = \frac{1}{12}(\textstyle\sum_{i=1}^{n} x_i b_i - \sum_{i=1}^{n} x_i a_i)^2 = \frac{1}{12}[\textstyle\sum_{i=1}^{n} x_i(b_i - a_i)]^2.$$

Since the nonnegativity of the term $[\sum_{i=1}^{n} x_i(b_i - a_i)]^2$, to minimize $\frac{1}{12}[\sum_{i=1}^{n} x_i(b_i - a_i)]^2$ is equivalent to minimize $\sum_{i=1}^{n} x_i(b_i - a_i)$.

Theorem 1 Let $x_1, x_2, \cdots, x_n$ be nonnegative decision variables and ξ_i be linear uncertain variable $L(a_i, b_i)$ with $a_i < b_i, i = 1, 2, \cdots, n$. Suppose that $\xi_1, \xi_2, \cdots, \xi_n$ are independent uncertain variables. Then for any scalar a and any confidence level $\alpha \in (0,1)$, the chance constraint

$$M\{\sum_{i=1}^{n} x_i\xi_i \geq a\} \geq \alpha$$

holds if and only if

$$\Phi(0) \leq 1 - \alpha$$

where $\Phi(x)$ is the uncertainty distribution of $x_1\xi_1 + x_2\xi_2 + \cdots + x_n\xi_n - a$.

Proof: Since ξ_i are assumed to be independent linear uncertain variables, the quantity

$$x_1\xi_1 + x_2\xi_2 + \cdots + x_n\xi_n - a$$

is also linear uncertain variable with parameters $a' = x_1a_1 + x_2a_2 + \cdots + x_na_n - a$ and $b' = x_1b_1 + x_2b_2 + \cdots + x_nb_n - a$. So the uncertainty distribution of $x_1\xi_1 + x_2\xi_2 + \cdots + x_n\xi_n - a$ is

$$\Phi(x) = \begin{cases} 0, & \text{if } x < a' \\ (x - a')/(b' - a'), & \text{if } a' \leq x \leq b' \\ 1. & \text{if } x > b' \end{cases}$$

Furthermore,

$$M\{\sum_{i=1}^{n} x_i\xi_i \geq a\} = M\{\sum_{i=1}^{n} x_i\xi_i - a \geq 0\} = 1 - M\{\sum_{i=1}^{n} x_i\xi_i - a \leq 0\}$$

Thus the inequality

$$M\{\sum_{i=1}^{n} x_i\xi_i \geq a\} \geq \alpha$$

is equivalent to the inequality

$$M\{\sum_{i=1}^{n} x_i\xi_i - a \leq 0\} \leq 1 - \alpha.$$

That is $\Phi(0) \leq 1 - \alpha$ which proves the theorem.

In this case, models (1) and (2) can be converted into its deterministic equivalents as follows,

$$\begin{aligned} &\max \sum_{i=1}^{n} x_i(a_i + b_i) \\ &\text{Subject to:} \\ &\Phi(0) \leq \alpha, \\ &x_1 + x_2 + \cdots + x_n = 1, \\ &x_i \geq 0,\ i = 1, 2, \cdots, n. \end{aligned} \tag{3}$$

or

$$\begin{aligned} &\min \sum_{i=1}^{n} x_i(b_i - a_i) \\ &\text{Subject to:} \\ &\Phi(0) \leq 1 - \alpha, \\ &x_1 + x_2 + \cdots + x_n = 1, \\ &x_i \geq 0,\ i = 1, 2, \cdots, n. \end{aligned} \tag{4}$$

4.2 Models for trapezoidal uncertain variable

If the return rates are all trapezoidal uncertain variables, Let ξ_i be (a_i, b_i, c_i, d_i), where

$a_i < b_i \leq c_i < d_i, i = 1, 2, \cdots, n$. Then $\sum_{i=1}^{n} x_i\xi_i$ is $(\sum_{i=1}^{n} x_ia_i, \sum_{i=1}^{n} x_ib_i, \sum_{i=1}^{n} x_ic_i, \sum_{i=1}^{n} x_id_i)$. In accordance with the properties of trapezoidal uncertain variable, we have

$$E[\sum_{i=1}^{n} x_i\xi_i] = (\sum_{i=1}^{n} x_ia_i + \sum_{i=1}^{n} x_ib_i + \sum_{i=1}^{n} x_ic_i + \sum_{i=1}^{n} x_id_i)/4 = \sum_{i=1}^{n} x_i(a_i + b_i + c_i + d_i)/4,$$

$$V[\sum_{i=1}^{n} x_i\xi_i] = \frac{4\alpha^2 + 3\alpha\beta + \beta^2 + 9\alpha\gamma + 3\beta\gamma + 6\gamma^2}{48} + \frac{[(\alpha - \beta - 2\gamma)^+]^3}{384\alpha}$$

where

$$\alpha = (\sum_{i=1}^{n} x_i b_i - \sum_{i=1}^{n} x_i a_i) \vee (\sum_{i=1}^{n} x_i d_i - \sum_{i=1}^{n} x_i c_i),\ \beta = (\sum_{i=1}^{n} x_i b_i - \sum_{i=1}^{n} x_i a_i) \wedge (\sum_{i=1}^{n} x_i d_i - \sum_{i=1}^{n} x_i c_i),$$

and $\gamma = \sum_{i=1}^{n} x_i c_i - \sum_{i=1}^{n} x_i b_i$.

Theorem 2 Let $x_1, x_2, \cdots, x_n$ be nonnegative decision variables and ξ_i be trapezoidal uncertain variable (a_i, b_i, c_i, d_i) with $a_i < b_i \le c_i < d_i, i = 1, 2, \cdots, n$ and $\xi_1, \xi_2, \cdots, \xi_n$ be independent. Then for any scalar a and any confidence level $\alpha \in (0,1)$, the chance constraint

$$M\{\sum_{i=1}^{n} x_i\xi_i \ge a\} \ge \alpha$$

holds if and only if

$$\Phi(0) \le 1 - \alpha$$

where $\Phi(x)$ is the uncertainty distribution of $\sum_{i=1}^{n} x_i\xi_i - a$.

Thus the models (1) and (2) can be changed into the following formulas,

$$\begin{aligned} &\max\ \sum_{i=1}^{n} x_i(a_i + b_i + c_i + d_i) \\ &\text{Subject to:} \\ &\Phi(0) \le \alpha, \\ &x_1 + x_2 + \cdots + x_n = 1, \\ &x_i \ge 0,\ i = 1, 2, \cdots, n. \end{aligned} \tag{5}$$

and

$$\begin{aligned} &\min\ V[x_1\xi_1 + x_2\xi_2 + \cdots + x_n\xi_n] \\ &\text{Subject to:} \\ &\Phi(0) \le 1 - \alpha, \\ &x_1 + x_2 + \cdots + x_n = 1, \\ &x_i \ge 0,\ i = 1, 2, \cdots, n. \end{aligned} \tag{6}$$

4.3 Models for normal uncertain variable

An uncertain variable ξ is called normal if it has a normal uncertainty distribution

$$\Phi(x) = (1 + \exp(\frac{\pi(e - x)}{\sqrt{3}\sigma}))^{-1}, x \in R,$$

denoted by $N(e, \sigma)$ where e and σ are real number with $\sigma > 0$. Suppose that the return rate of ith security is normally distributed with parameters e_i and $\sigma_i > 0, i = 1, 2, \cdots, n$. Then we have

$$E[\sum_{i=1}^{n} x_i\xi_i] = \sum_{i=1}^{n} x_i e_i,\quad V[\sum_{i=1}^{n} x_i\xi_i] = (\sum_{i=1}^{n} x_i\sigma_i)^2.$$

Theorem 3 Assumed that $x_1, x_2, \cdots, x_n$ be nonnegative decision variables and $\xi_1, \xi_2, \cdots, \xi_n$ are independently uncertain variables with expected values $e_1, e_2, \cdots, e_n$ and variance ${\sigma_1}^2, {\sigma_2}^2, \cdots, {\sigma_n}^2$, respectively. Then for any scalar a and α, the chance constraint

$$M\{\sum_{i=1}^{n} x_i\xi_i \ge a\} \ge \alpha$$

Holds if and only if

$$\sum_{i=1}^{n} x_i(e_i + \sigma_i\Phi^{-1}(1 - \alpha)) \ge a$$

where Φ is the standardized normal distribution , i.e.,

$$\Phi(x) = (1 + \exp(-\frac{\pi x}{\sqrt{3}}))^{-1},\ x \in R.$$

Proof: Since ξ_i are assumed to be independently normal uncertain variables, the quantity

$$y = \sum_{i=1}^{n} x_i\xi_i - a$$

is also normal uncertain variable with the following expected value and variance,

$$E[y] = \sum_{i=1}^{n} x_i e_i - a,\ \ V[y] = (\sum_{i=1}^{n} x_i\sigma_i)^2.$$

We note that

$$\frac{(\sum_{i=1}^{n} x_i\xi_i - a) - (\sum_{i=1}^{n} x_i e_i - a)}{\sum_{i=1}^{n} x_i\sigma_i}$$

must be standardized normal uncertain variable. Since the inequality

$$\sum_{i=1}^{n} x_i\xi_i \geq a$$

is equivalent to

$$\frac{(\sum_{i=1}^{n} x_i\xi_i - a) - (\sum_{i=1}^{n} x_i e_i - a)}{\sum_{i=1}^{n} x_i\sigma_i} \geq \frac{0 - (\sum_{i=1}^{n} x_i e_i - a)}{\sum_{i=1}^{n} x_i\sigma_i}$$

We have

$$M\{\eta \geq -\frac{(\sum_{i=1}^{n} x_i e_i - a)}{\sum_{i=1}^{n} x_i\sigma_i}\} \geq \alpha$$

where η is the standardized normal uncertain variable. This inequality holds if and only if

$$\sum_{i=1}^{n} x_i(e_i + \sigma_i\Phi^{-1}(1-\alpha)) \geq a\,.$$

The theorem is proved.

Under the conditions, the models (1) and (2) may be formulated as the following linear equivalents,

$$\begin{aligned} &\max \sum_{i=1}^{n} x_i e_i \\ &\text{Subject to:} \\ &\sum_{i=1}^{n} x_i(e_i + \sigma_i\Phi^{-1}(\alpha)) \geq a, \\ &x_1 + x_2 + \cdots + x_n = 1, x_i \geq 0,\ i = 1,2,\cdots,n. \end{aligned} \tag{7}$$

and

$$\begin{aligned} &\min \sum_{i=1}^{n} x_i\sigma_i \\ &\text{Subject to:} \\ &\sum_{i=1}^{n} x_i(e_i + \sigma_i\Phi^{-1}(1-\alpha)) \geq a, \\ &x_1 + x_2 + \cdots + x_n = 1, \\ &x_i \geq 0,\ i = 1,2,\cdots,n. \end{aligned} \tag{8}$$

Thus we can solve the models (3)-(8) by traditional methods.

5. Numerical Examples

Example 2 Assume that there are 6 securities. Among them, returns of the six securities are all normal uncertain variables $\xi_i = N(e_i, \sigma_i),\ i = 1, 2, 3, 4, 5, 6$. Let the return rates be

$$\xi_1 = N(-1,1),\ \xi_2 = N(0,1),\ \xi_3 = N(1,2), \xi_4 = N(2,1), \xi_5 = N(3,2),\ \xi_6 = N(4,3)\,,$$

Then

$$\sum_{i=1}^{6} x_i\xi_i = N(-x_1 + x_3 + 2x_4 + 3x_5 + 4x_6,\ x_1 + x_2 + 2x_3 + x_4 + 2x_5 + 3x_6)$$

Thus, we have

$$\begin{aligned} E[\sum_{i=1}^{6} x_i\xi_i] &= -x_1 + x_3 + 2x_4 + 3x_5 + 4x_6\,, \\ V[\sum_{i=1}^{6} x_i\xi_i] &= x_1 + x_2 + 2x_3 + x_4 + 2x_5 + 3x_6\,. \end{aligned}$$

Suppose that the confidence level $\alpha = 0.05$, and the minimum excepted return the investor can accept is $a = -0.1$, then $\Phi^{-1}(0.05) = -1.62$. Thus the models (7) is the following:

$$\begin{aligned} &\max\ -x_1 + x_3 + 2x_4 + 3x_5 + 4x_6 \\ &\text{Subject to:} \\ &2.62x_1 + 1.62x_2 + 2.24x_3 - 0.38x_4 + 0.24x_5 + 0.86x_6 \leq 0.1, \\ &x_1 + x_2 + \cdots + x_6 = 1, x_i \geq 0,\ i = 1,2,\cdots,6 \end{aligned} \tag{9}$$

By use of Matlab 7.0 on PC we obtain the optimal solution of model (9). The optimal solution of model (9) is

(0.0000,0.0000,0.0000,0.4907,0.2444,0.2649)

and the optimal value of the objective function is 2.7742. This means that in order to gain maximum expected return with the risk not greater than -0.1 at the confidence level 0.05, the investor should assign his money according to the optimal. The corresponding maximum expected return is 2.7742.

In model (8), if the investor gives the preset total return rate is $a = 0.5$ and the preset confidence level is $\alpha = 0.9$, then the model (8) is the following,

$$\begin{aligned} &\min \ \ x_1 + x_2 + 2x_3 + x_4 + 2x_5 + 3x_6 \\ &\text{Subject to:} \\ &2.2x_1 + 1.2x_2 + 1.4x_3 - 0.8x_4 - 0.6x_5 - 0.4x_6 \le -0.5, \\ &x_1 + x_2 + \cdots + x_6 = 1, x_i \ge 0, \ i = 1, 2, \cdots, 6. \end{aligned} \tag{10}$$

we obtain the optimal solutions of model (10) is

$$(0.0091, 0.1131, 0.0000, 0.8778, 0.0000, 0.0000),$$

and the value of objective function is 1.0000. This means that in order to minimize the risk with the return rate not less than 0.5 at the confidence level 0.9, the investor should assign his money according to the optimal. The corresponding minimum risk is 1.0000.

6. Conclusions

In this paper, uncertain variable is applied to portfolio selection problems, and two types of uncertain programming models for portfolio selection with uncertain returns on basis on the uncertain theory are provided. In order to solve the proposed models by traditional methods we discuss the crisp equivalents when the uncertain returns are chosen to be some special uncertain variables and give two examples to explain the efficiency of the method. The paper does not include the conditions when the return rates are general uncertain variables, this can be interesting areas for future researches.

References

A. Charnes, W.W. Cooper. (1965). Chance-constrained programming. *Management Science* 6, 73-79.

B. Liu. (2009). Uncertainty theory. [Online] Available: http://orsc.edu.cn/liu.

B.Liu. (2002). Theory and practice of uncertain programming. Physics-verlag, Heidelberg.

H. Markowitz. (1952). Portfolio selection, *Journal of finance*, 7, 77-91.

H. Markowitz. (1959). Portfolio selection: Efficient diversification of investments, Wiley, New York.

J.O. Williams. (1997). Maximizing the probability of achieving investment goals. *Journal of portfolio management* 24, 77-82.

P.L. Brockett, A. Charnes, W.W. Cooper, K.h. Kwon, T.W. Ruefli. (1992). Chance-constrained programming approach to empirical analysis of mutual fund investment strategies. *Decision Science,* 23, 385-408.

S.X. Li, Z. Huang. Determination of the portfolio selection for a property-liability insurance company. *European Journal of operational research,* 88, 257-268.

S.X. Li. (1995). An insurance and investment portfolio model using chance constrained programming. *International Journal of management science,* 23, 577-585.

Modern Applied Science
www.ccsenet.org/journal.html
Vol. 3, No. 9
September 2009

Pattern Synthesis of Sparse Phased Array Antenna Using Genetic Algorithms

Rongcang Han
Department of Physics, Linyi Normal University, Linyi 276005, China
E-mail: hanrongcang@lytu.edu.cn

Abstract

Sparsely sampled irregular arrays and random arrays have been used or proposed in several fields such as radar, sonar, and ultrasound imaging. One method of pattern synthesis for sparse phased array antenna using genetic algorithms is introduced. We start with an introduction to genetic algorithms and then consider the problem of finding the best amplitude layout of elements in sparse arrays. The optimization criteria are then reviewed: creation of beam patterns with low main lobe width and low side lobes.

Keywords: Genetic Algorithms, Sparse Array Antenna, Phased Array, Pattern Synthesis

1. Introduction

Making an array sparse means turning off some elements in a uniformly spaced or periodic array to create a desired amplitude density across the array aperture. An element connected to the feed network is "on", and an element connected to a matched or dummy load is "off". Making an array sparse to produce low side lobes is much simpler than the more general problem of non-uniform spacing the elements. Non-uniform spacing has an infinite number of possibilities for placement of the elements. Making an array sparse has 2^Q possible combinations, where Q is the number of array elements. If the array is symmetric, then the number of possibilities is substantially smaller. Making an array sparse may also be thought of as quantized amplitude taper where the amplitude at each element is represented by one bit.

Traditional optimization techniques searching for the best solutions usually use gradient methods or random searching. Gradient methods are efficient, but have disadvantages of getting stuck in local minima, requiring gradients calculations, working only on continuous parameters. Random-search methods don't require gradient calculations, but tend to be slow, and susceptible to getting stuck in local minima. Genetic algorithm optimizer is robust global search method. Its research is based on probability, having advantage of avoiding getting stuck in local minima(Haup,1994,p993).

2. Genetic Algorithms

This section is a quick overview of genetic algorithms, much more detail on genetic algorithms is found in the book of Holland (Holland, 1992). Gene is the basic building blocks of genetic algorithms. A gene is binary encoding of a parameter. In computer algorithm, a chromosome is an array of genes, a number of chromosomes make up one population. Each chromosome has an associated fitness function, assigning a relative merit to that chromosome. The algorithm begins with a large list of random chromosomes. Fitness functions are evaluated for each chromosome. The chromosomes are ranked from the most-fit to the least-fit, according to their respective fitness functions. Unacceptable chromosomes are discarded, leaving a superior species-subset of an original list, which is the process of selection. Genes that survive become parents, by crossing over some of their genetic material to produce two new offspring. The parents reproduce enough to offset the discarded chromosomes. Thus, the total number of chromosomes remains constant after every iteration. Mutations cause small random changes in a chromosome. Fitness functions are evaluated for the offspring and mutated chromosome, and the process is repeated. The algorithm stops after a set number of iterations, or when an acceptable solution is obtained. Figure1 is a flow chart of genetic algorithms. (Diógenes Marcano and Filinto Durán, 2000, p13).

A sparse array has discrete parameters. One bit represents the element state as "on" = 1 or "off "= 0. For example, an eight element array may be represented by 10110101, where elements 2 and 5 are turned "off." Assuming the linear array is symmetric about its center allows the 2N element array to be represented by a gene with N bits. Our six-element

array example can then be represented by the gene 101. The fitness associated with this gene is the maximum relative side lobe level (rsll) of its associated far-field pattern. The function in this paper is the relative far-field pattern of an array of point sources. Its output to be minimized is the maximum rsll. The parameters affecting the output are whether an antenna element is on or off.

3. Method

Suppose we consider an array of antenna elements uniformly spaced in a straight line along the z axis. The far-field radiation pattern produced by such an array may be expressed as

$$E(\theta,\varphi)=\sum_{n=0}^{N-1} I_n EP_n(\theta,\varphi)e^{j(nkd\cos\theta+\beta_n)} \tag{1}$$

where I_n are the current amplitudes of element excitations, $\beta_n=-nkd\cos\theta_0$, θ_0 is the angle that the main beam of the antenna directed to. $EP_n(\theta,\varphi)$ are the individual array element patterns, k=2π/λ is the free-space wave number, d is the separation distance between elements.

Now the main process of antenna synthesis in genetic algorithms is given below.

A. Establish decision variable and constraint condition, then encoding them.

$$I_n=\begin{cases}1 & on\\ 0 & off\end{cases} \tag{2}$$

B. Create optimization pattern:

$$\min E_{mt}=\left[\frac{1}{Q}\sum_{i=1}^{Q}|e_i|^2\right]^{\frac{1}{2}} \tag{3}$$

Where

$$e_i=\frac{T_i-F_i}{T_i}, i=1,2,\cdots,Q \tag{4}$$

T_i is the level of the desired radiation pattern at the point Q, and F_i is the level of the pattern generated by genetic algorithms.

C. Define fitness function:

$$F_m=\frac{1}{1+E_{mt}^{\alpha}} \tag{5}$$

where $\alpha\in(0,1]$. Figure2 shows the behavior of the fitness as a function of the error. We can see that the algorithm favors individuals with a high fitness. (Daniel, 2005, p358).

4. Numerical Illustration

Here, genetic algorithms is used to minimize the maximum side lobe level for an array with aperture L= 40λ (total number of elements is 81) with 35 active elements lying on a grid with λ/2 element distance. In this problem, our goal is to get minimum side lobe level. A best layout of elements is given below by genetic algorithms. The symmetric amplitude of the array can be used to making scanning beam. The pattern of this array is given in figure3. The pattern when the array scanning is shown in figure4. The layout of the elements is shown by a string of bits below.

5. Conclusions

This paper introduced the use of genetic algorithms for sparse linear arrays to obtain scanning beam. The beauty of the genetic algorithm is that it can optimize a large number of discrete parameters. The genetic algorithm intelligently searches for the best layout of element amplitude intelligently searches for the best layout of element amplitude that produces low side lobes.

Many additional extensions are possible, including thinning circular arrays, planar arrays with directional elements, scanning planar arrays, etc.

References

Daniel W. Boeringer and Douglas H. Werner. (2005). A Simultaneous Parameter Adaptation Scheme for Genetic Algorithms with Application to Phased Array Synthesis. *IEEE Transactions on antennas and Propagation*, Vol. 53, No. 1, 356-371.

Diógenes Marcano and Filinto Durán. (2000). Synthesis of Antenna Array Using Genetic Algorithms. *IEEE, Antennas*

and Propagation Magazine, Vol. 42, No. 3, 12~20.

Holland J.H. (1992). *Adaptation in Nature and Artificial Systems*. *MIT Press*, 1992.

Randy L, Haupt. (1994). Arrays Using Genetic Algorithm. *IEEE Transactions on Antennas and Propagation*, Vol. 42, No. 7, 993~999.

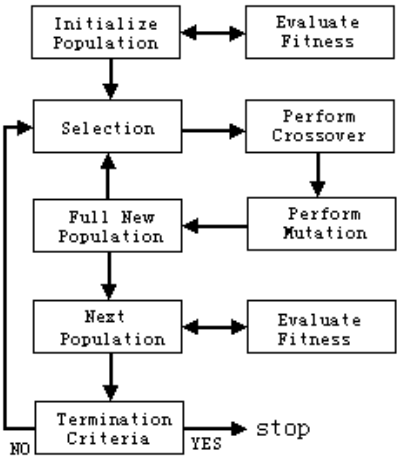

Figure 1. A flow chart of genetic algorithms

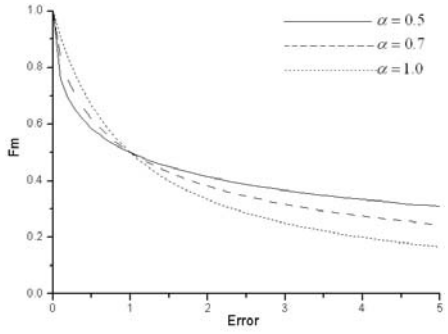

Figure 2. A plot of fitness function versus error

1 0 0 0 0 0 0 1 0 0 0 0 0 1 0 0 0 0 1 0 0 0 0 1 0 0 1 1 0 1 1 0 1 1 1 1 1 1 1 1, 1,
1 1 1 1 1 1 1 1 0 1 1 0 1 1 0 0 1 0 0 0 0 1 0 0 0 0 1 0 0 0 0 0 1 0 0 0 0 0 0 1
Sidelobe Peak: -12.4 [dB]

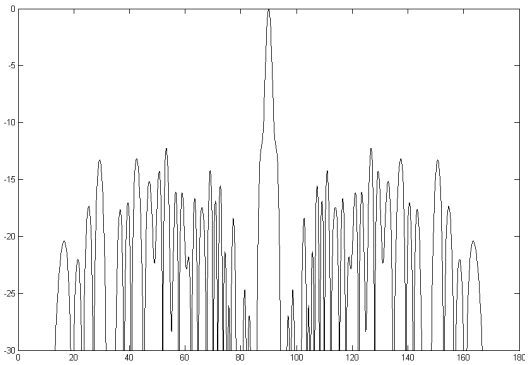

Figure 3. Result of non-scanning pattern of genetic algorithms

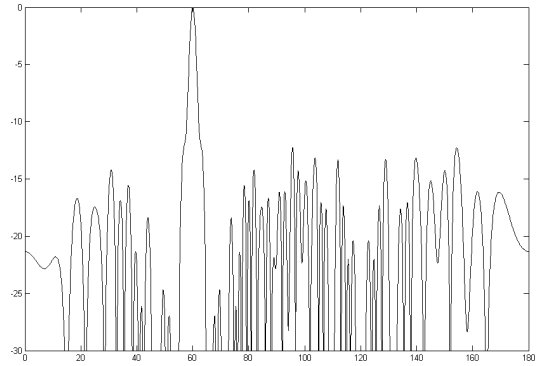

(a) $\theta_0 = 60^\circ$

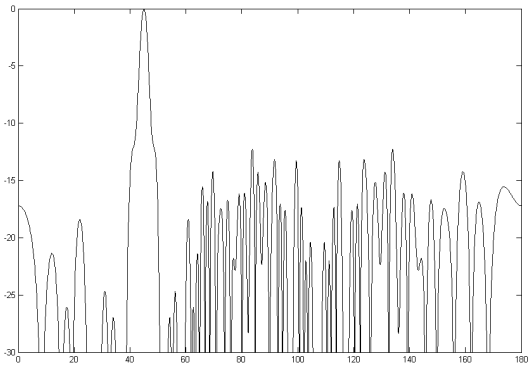

(b) $\theta_0 = 45^\circ$

Figure 4. Radiation patterns of the phased array with different scanning angles

Modern Applied Science
www.ccsenet.org/journal.html
Vol. 3, No. 9
September 2009

The Performance Study of Hybrid-driving Differential Gear Trains

Lei Wang, Jiancheng Yang & Xiaoqin Han
School of Mechanical and Electronic Engineering
Tianjin Polytechnic University, Tianjin 300160, China
E-mail: wangleioa01@163.com

Abstract

This article in view of the differential gear trains theory characteristic, carried on the analysis to the mechanism performance, and obtained the best design scheme of the Hybrid-driving two degree of freedom differential gear trains. Adopted programmable logic controller (short for PLC) component and frequency converter to control the constant speed motor and the variable speed motor, developed a laboratory bench of Hybrid-driving two degree of freedom differential gear trains and utilized a encoder to gather the experimental data under this condition. This laboratory bench will be used as a research platform for basic theory of textile machinery and providing the rationale to optimize its variable speed mechanism.

Keywords: Hybrid-driving, Two degree of freedom, Differential gear trains, PLC

1. Introduction

The Hybrid-driving mechanism both has the high efficiency and the high bearing capacity of traditional mechanism, and it has the merit of flexibility and adjustability of controllable drive mechanism. The system research of Hybrid-driving began in the early 90s by the British scholar Tokuz who first proposed the concept of Hybrid machine(Tokuz LC,1992,p.23-35). Interiorly, there also appeared some Hybrid-driving research(Liu,Jianqin,2000,p.157-198 &Cheng, Guangyun,1990,20(3),p.64-67),but the Hybrid-driving study of differential gear trains were few, in general to study most about the multi-degree of freedom link mechanism.

In domestic and abroad, differential gear trains as the gear trains of two degrees of freedom had been researched bounteously, and mainly concentrated in its transmission ratio, efficiency and power flow. Mathis Roland had carried on the theoretical analysis to differential gear trains about its each kind of computation; Heng Sun had a detailed study to the differential gear trains about its force and efficiency(Sun,heng,1990, p.247-264); Baoxian Jia and others analyzed the power flow and meshing efficiency of the 2K-H differential gear trains(Jia,Baoxian & Bian,Wenfeng, 1999, 16(05), p. 12-15); Shaolie Cao had a research about the movement of the 2K-H differential gear trains under the inotropic effect(Cao,Shaolie,1997,p.28-36).

At first, this article made a detailed description on kinematic analysis to the differential gear trains, and obtained the relationship between speed and torque of the input/output side of 2K-H type differential gear trains; Followed, this article conducted a systematic study of coordination and control; Finally, based on an analysis of the result ,this subject designed the experimental device parameter and a test-bench of Hybrid-driving differential gear trains, and accomplished the selection and debugging of hardware and software on the test-bench, and obtained some valuable data.

2. The overview of differential gear trains

The differential gear trains are a kind of epicyclic gear trains and are a two degree of freedom epicyclic gear trains. As shown in Figure 1 is a common 2K-H type differential gear trains. Among the three basic components (both center gears, a tie bar), two components must be given the track of its movement in order to derive the third component. The input components have a variety of combinations. The differential gear trains has a stable transmission and a high precision and many other merits, .it widely applies in textile machinery and vehicles and other engineering machinery.

3. Fundamental equations of differential gear trains

Shown in Figure 1 for the 2K-H type differential gear trains, if we take tie bar H for the reference system to observe this mechanism movement, then, relative to the tie bar H, the movement of planetary gear P is fixed axis rotation, and

because center gear A and B is coaxial line with tie bar H, therefore relative to the tie bar, the movement of two gears are also fixed axis rotation. Thus, when we analyze the epicyclic gear trains, if we take the tie bar as reference system to observe the movement of epicyclic gear trains, then this epicyclic gear trains on into "fixed axis gear trains" which is considerable with itself,this is known as conversion mechanism of epicyclic gear trains. In this case, the angular velocity of various components in conversion mechanism, namely, relative to the tie bar H, the angular velocity of various components are as follows:

$$\text{Gear A: } \omega_A^H = \omega_A - \omega_H$$

$$\text{Gear B: } \omega_B^H = \omega_B - \omega_H$$

$$\text{Tie bar H: } \omega_H^H = \omega_H - \omega_H = 0$$

Due to the transformation mechanism is fixed axis gear trains, therefore, its transmission ratio can be determined according to the calculation method of fixed axis gear trains, consequently:

$$i_{AB}^H = \frac{\omega_A^H}{\omega_B^H} = \frac{\omega_A - \omega_H}{\omega_B - \omega_H} = -\frac{z_B}{z_A} \tag{1}$$

In the formula: A, B are the central gear, H is tie bar; i_{AB}^H is the transmission ratio between the two center gears A and B, according to the transmission ratio of fixed axis gear trains to determine; ω_A is the rotational speed of center gear A, ω_B is the rotational speed of center gear B, ω_H is the rotation speed of tie bar H; ω_A^H is the relative velocity which is the central gear A relative to the tie bar H; ω_B^H is relative velocity which is the central gear B relative to the tie bar H.

By the formula (1), we can see, if we know any two Parameters among ω_A, ω_B, ω_H will be able to find the another. In other words, setting the two input rotational speed will be able to determine the output rotational speed .Therefore, the differential gear trains is two degree of freedom mechanism.

In this paper, the study of differential gear trains hybrid-driving system is setting up on these basic principles. Constant speed of main motor and control motor as two power input mechanism to realize controllable output of the third component of the differential mechanism.

4. Kinematic Analysis of Differential Gear trains

The Hybrid-driving differential gear trains have two inputs and one output. It respectively connect with the constant speed motor, the control motor and the output load, if according to the known parameters of constant speed motor, control motor and the load to design differential gear trains, first we must analyze the relationship between the torque and the speed of the I/O in the differential gear trains.

In this paper, the meaning of hybrid-drive differential gear trains is an entire system, which includes differential gear trains and other retarding mechanism as well as belt transmission. Accurately speaking, in the overall system, the transmission part and the mechanical parts are composed of the differential gear trains, constant speed motor, control motor and the decelerate gear cluster of output load.

4.1 The angular velocity analysis of differential gear trains

In order to clear the relationship of rotational speed of input and outputs, we set up a rotational speed model diagram to analyze the differential gear trains (as shown in Figure 2).

It is the part of structure diagram (shown in figure 3) of 2K-H type differential gear trains which had been studied in my subject. Thereinto, the planet carrier H is gear 5, gear 1 and gear 4 are center gears, gear 2 and gear 3 are symmetrical planetary gears. The main axis drive center gear 1 rotation, the axis 1 installs on planet carrier H, drive planetary gears 2 and 3 rotation. The center gear 4 is gear shaft, and set up at the main axis.

According to the basic principle of differential gear trains, we can educe its transmission ratio relationship (as shown in Figure 3):

$$i_{14}^h = \frac{\omega_1 - \omega_h}{\omega_4 - \omega_h} = \frac{z_4 \cdot z_2}{z_1 \cdot z_3} \tag{2}$$

In formula: i_{14}^h ------differential gear transmission ratio;

ω_1 ------the rotational speed of center gear 1;

ω_h ------the rotational speed of planet carrier H;

ω_4 -------the rotational speed of center gear 4;

z_1, z_2, z_3, z_4 for the gear;

We can see from the formula (2) that when the structure of differential gear trains is determined, In other words, when z_1, z_2, z_3, z_4 are known, the differential gear trains transmission ratio i_{14}^h is a constant. Once the structure is determined, the transmission ratio will be determined too, but has nothing to do with the input speed.For the sake of brevity, makes $i_{14}^h = k$, then ,there is:

$$\frac{\omega_1 - \omega_h}{\omega_4 - \omega_h} = k \tag{3}$$

1) center gear 1,4 as input and tie bar H as output, then,

$$\omega_h = f(\omega_1, \omega_4) = \frac{1}{1-k}\omega_1 - \frac{k}{1-k}\omega_4 \tag{4}$$

2) center gear 1 and tie bar H as input, center gear 4 as output, then,

$$\omega_4 = f(\omega_1, \omega_h) = \frac{1}{k}\omega_1 + \frac{k-1}{k}\omega_h \tag{5}$$

3) center gear 4 and tie bar H as input, center gear 1 as output, then,

$$\omega_1 = f(\omega_4, \omega_h) = k \cdot \omega_4 + (1-k) \cdot \omega_h \tag{6}$$

4.2 The torque analysis of differential gear trains

It is similar with the analysis of the rotational speed relationship of differential gear trains, to establish the torque analysis model diagram of differential gear trains (shown in Figure 4). This diagram appropriately transforms the reduction ratio to directly express the torque of the constant speed of main motor, control motor and output load at input / output three sides on differential gear trains. Only to analyse the torque relationship of the differential gear trains can obtain the torque relationship of the constant speed motor, the control motor and the output load.

Here do not consider the friction when we analyze torque relationship of the differential gear trains, the main purpose is to analyze the major questions. In order to solve the problem conveniently, we make the following hypothesis: (1) Only to consider the torque generated by the circumferential force which is the role by inter-gear; (2) No matter how many planetary gears to participate the transmission, regarding the transmission of all the load are finished by one planetary gear; (3) To consider all the force are on the same plane.

First, it is necessary to clarify a question: As mentioned above, the differentia gear trains is a two degree of freedom structure. The speed of the third client can be unique determined when we give the speed of arbitrary at both ends. Then, whether the torque of differential gear trains also has the similar nature?

After assigning the speed of both ends of differential gear train, we can only give one of the driving moment of one side, but the moment of the other end is possibly the driving moment, or is the resistance moment to nature counterbalance, this should accord to the specific circumstances of the mechanism themselves to confirmation, but can not be assigned casually. Generally, it is easy to have such illusion: the differential gear trains are two degrees of freedom, then you can give any one of two basic components with any angular velocity and moment. In fact, this idea is wrong. Because the three components of differential gear trains possess balance principle of outside moment. Consequently:

$$M_1 + M_4 + M_h = 0 \tag{7}$$

In formula: M_1 ----the torque of center 1; M_4 ----the torque of center 4;

M_h ----the torque of planetary gear;

As for the uniform rotation of the differential gear trains, there exist a balanced relationship between the input power and output power,

$$M_1\omega_1 + M_4\omega_4 + M_h\omega_h = 0 \tag{8}$$

From the formulae (7), (8) and (3), we can obtain the torque relationship, as follows:

(1) the center gear 1 and 4 as input, tie bar H as output,

$$\begin{cases} M_1 = \dfrac{1}{k-1}M_h \\ M_4 = \dfrac{-k}{k-1}M_h \end{cases} \tag{9}$$

(2) the center gear 1 and the tie bar H as input, the center gear 4 as output,

$$\begin{cases} M_1 = -\dfrac{1}{k}M_4 \\ M_h = \dfrac{1-k}{k}M_4 \end{cases} \tag{10}$$

(3) the center gear 4 and the tie bar H as input, the center gear 1 as output,

$$\begin{cases} M_4 = -kM_1 \\ M_h = (k-1)M_1 \end{cases} \tag{11}$$

By formulae (9),(10) and (11) ,we can see that if we know the size of a differential gear trains mechanism, then we can determine the size of the other under known the two input rotational speed and a driving moment.

5. To determine the program of differential gear trains

The differential gear trains shows in the Figure 3, through the rotational speed analysis and torque analysis, we can see that there are three programs to achieve hybrid-driven. Which kind of program is reasonable and reliable? Next, from the aspect of torque to analyze the feasibility of every program, and put the results of the analysis as basis for designing differential gear trains and determining its structure.

Because this differential gear trains is outside mesh, its gear ratio must be greater than zero. This is an important prerequisite to analyse the mechanism.

(1) the center gear 1 and 4 as input, tie bar H as output,

By (9)-type,when $k > 0$,the two coefficient of $\frac{1}{k-1}$ and $\frac{-k}{k-1}$ are opposite, and also regarding one of the two torque M_1 and M_4 must be same direction with the output torque. In other words, one of the two torque M_1 and M_4 is impetus and the other is resistance, so we can see that this program is infeasible.

(2) the center gear 1 and the tie bar H as input, the center gear 4 as output,

By (10)-type, when 0<k<1, the input torque M_1 and M_4 are opposite direction, M_4 and M_h are same direction. In other words, M_1 is impetus and M_4 is resistance. When $k > 1$, M_1 and M_h are opposite direction with M_4. In other words, M_1 and M_h are impetus. So this program is feasible.

(3) the center gear 4 and the tie bar H as input, the center gear 1 as output,

By (11)-type, When $k > 1$, M_1 and M_h are opposite direction with M_4, M_1 and M_h are impetus. Under this condition, because of $M_4 = -kM_1$, Whether the input side connect with constant speed motor or control motor, we must provide K times the output torque, which is obviously infeasible.

From the above analysis, we can see that it is feasible for center gear and tie bar as input and the another center gear as output. This paper takes into account the factors of design, machining and cost of the deceleration gear trains of the I/O port. Finally, we determined the program 2 as our research object.

From the previous analysis, we can see that the transmission ratio $k>1$ is to meet the requirement. Once the K is determined, the structure of differential gear train is determined too. According to the rotational speed model (shown in Figure 2), we can transform the (5)-type into the new form, as below:

$$i_o\omega_o = \frac{1}{k}\cdot\omega_c / i_c + \frac{k-1}{k}\cdot\omega_v / i_v \tag{12}$$

In formula: i_c ------the transmission ratio of constant speed input port;

i_v ------the transmission ratio of variable speed input port;

i_o ------the transmission ratio of output port;

ω_o ------the rotational speed of output port;

ω_c ------the rotational speed of constant input port;

ω_v ------the rotational speed of variable input port;

k ------- the transmission ratio of differential gear trains

Then, the rotational speed relationship between output port and constant speed motor and variable speed motor is as below:

$$\omega_o = \frac{1}{ki_oi_c}\omega_c + \frac{k-1}{ki_vi_c}\omega_v \tag{13}$$

According to the torque model shown in Figure 4, we can transform the (10)-type into the new form, as below:

$$\begin{cases} i_c M_c = -\dfrac{1}{k} M_o / i_o \\ i_v M_v = \dfrac{1-k}{k} M_o / i_o \end{cases} \tag{14}$$

In formula: M_C ---the torque of constant port; M_V ---the torque of variable port;

M_O ---the torque of output port;

Then, the output torque of constant speed motor: $M_c = -\dfrac{1}{k i_c i_o} M_o$

the output torque of variable speed motor: $M_v = \dfrac{1-k}{k i_v i_o} M_o$

6. The design of control system

6.1 The system hardware

The main hardware include a PLC, two frequency converters, two three-phase asynchronous motors, a transducer and a display. The concrete hardware are as follows: (1) DVP-20EX PLC as the core of system control, this PLC has two communication interfaces (rs-485 and rs-232).RS-485 can directly communicate with the frequency converters; RS-232 can communicate with the computer through the connecting line, which one side is a circular 8-pin interface, and the other side is needle-shaped 9-pin D-type interface. (2)The frequency converter selects VFD007B43A, its input: three-phase, 380-480VAC 50/60HZ; its output: the range of frequency is 0.1- 400HZ; the temperature of environment: -10 to 50 degree Centigrade. (3)Three-phase asynchronous motor, rated speed: 1380rad/min; Power: 0.6KW; Voltage: 380V; Electric current: 1.59A. (4)Sensor, it is to detect the actual rotational speed of output port. (5) display, it is to display the output port actual rotational speed.

6.2 The system of software

One PLC controls the two frequency converters to drive the two three-phase asynchronous motor respectively in this system. So that, one motor is constant speed and the other is variable speed. At the same time, installing a sensor on the output side to detect the actual rotational speed of the output port. PLC program flow diagram is in Figure 5, below:

7. Experimental results

The known transmission parameters of gear and belt of the test bench, as shown in the table 1.Based on these parameters, we can calculate the theoretical value of output-port of the hybrid-driving differential gear trains.

In the experimental process, the constant speed motor takes four fixed speed, they are 0 r / min, 330 r / min, 630 r / min and 930 r / min. The range of variable speed motor is from forward 1380r / min to reverse 1380 r/ min. When the two-motor run steadily, the constant speed motor takes a fixed speed, and change the speed of variable speed motor under this condition. At the same time, we record the actual speed of output-port. The actual value and theoretical value of the output-port are shown in the table 2 below. The negative mean reverse in the form 2. (Look from the right side of the test-bench, the output-port clockwise direction is forward.)

According to the experimental data in the table 2, we can see that the actual rotational speed of the motor is lower than its rated rotational speed, so it causes the actual rotational speed of output-port is less than its theoretical value. But generally speaking, the actual value and the theoretical value are quite close, this shows that the test-bench have achieved the anticipated request. This test-bench provides a good experimental platform for the basic theory research in the future.

8. Conclusion

Through researching the theory of hybrid-driving differential gear trains and carring out experiment many times on the designed test-bench,finally, this article obtains two conclusions:

(1)This paper designed a test-bench of hybrid-driving two degree of freedom differential gear trains, and its mechanical properties are reliable and stable,low noise, smooth running. Generally speaking, it is able to achieve the anticipated purpose.

(2)This test-bench uses PLC component to enable system control more precise, easy operation, debugging easy, gathering the data accurately and conveniently. It provides a good experimental platform for the basic theory research in the future.

References

Cao, Shaolie. (1997). 2K-H differential gear trains inotropic effect in the actuall movement. *Journalof Wuhan*

Transportation University of Science and Technology, (5): 28-36.

Cheng, Guangyun. (1990). Two degrees of freedom planar linkage mechanisms achieve precise trajectory study. *Journal of Southeast University,* 20(3), 64-67.

Jia, Baoxian & Bian, Wenfeng. (1999). 2K-H differential gear trains power flow and meshing efficiency. *Journal of mechanical design,* 16(05), 12-15.

Liu, Canjun. (2004). *Practical sensor*. Beijing: National Defense Industry Publishing House. (Chapter 3).

Liu, Jianqin. (2000). Elastic linkage precision trajectory control Generative Theory and Experimental study. Tianjin:Tianjin University.

P.R. Ouyang & Q. Li. (2004). Design modeling and control of a hybrid machine system. *Mechatronics*14 (1197-1217).

Sun, Heng. (1990). *Mechanical principle*.(2rd ed.). Beijing:Higher Education Publishing House. (Chapter 5).

Tokuz LC. (1992). Hybrid machine modeling and control. *International Journal of Automation and computing,* 3(3), 23-35.

Table 1. The transmission parameters of gear and belt

gear	m	z
1	1.75	67
2	1.75	23
3	1.75	30
4	1.75	60
5	2.5	20
6	2.5	100
7	2	20
8	2	35
belt transmission	2:1	

Table 2. the actual speed of output-port of hybrid-drive differential gear trains

contact speed (rad/min)	variable speed (rad/min)	actual speed (rad/min)	theoretical speed (rad/min)	contact speed (rad/min)	variable speed (rad/min)	actual speed (rad/min)	theoretical speed (rad/min)
930	1380	48.96	54.61	330	1180	-40.13	-43.65
930	1180	65.28	72.87	330	980	-18.58	-25.39
930	980	73.34	91.1304	330	780	-2.76	-7.13
930	780	102.52	109.39	330	580	5.64	11.13
930	580	125.10	127.65	330	380	24.98	29.39
930	380	132.86	145.91	330	-380	89.47	98.78
930	0	176.67	180.61	330	-580	108.52	117.04
630	1380	-1.93	-3.65	0	1380	-109.24	-126.00
630	1180	10.59	14.61	0	1180	-91.60	-107.74
630	980	22.64	32.87	0	980	-73.98	-89.48
630	780	46.28	51.13	0	780	-63.15	-71.26
630	580	61.12	69.39	0	580	-41.30	-52.96
630	380	78.23	87.65	0	380	-23.76	-34.69
630	-380	140.00	157.04	0	-380	33.40	34.69
630	-580	168.87	175.30	0	-580	48.65	52.96
330	1380	-53.81	-61.91	0	-780	66.82	71.22

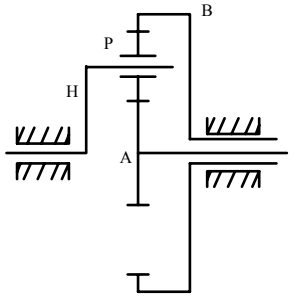

Figure 1. planetary differential gear trains structure diagram

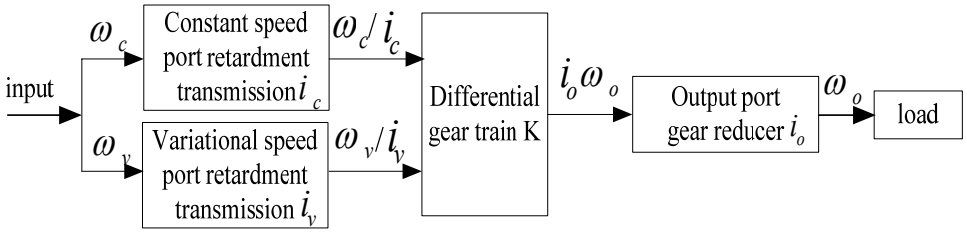

Figure 2. Hybrid drive differential gear train rotational speed analysis

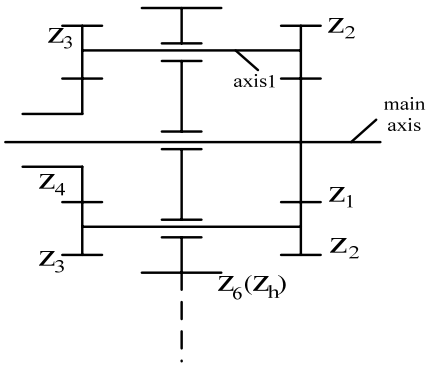

Figure 3. structural diagram of differential gear

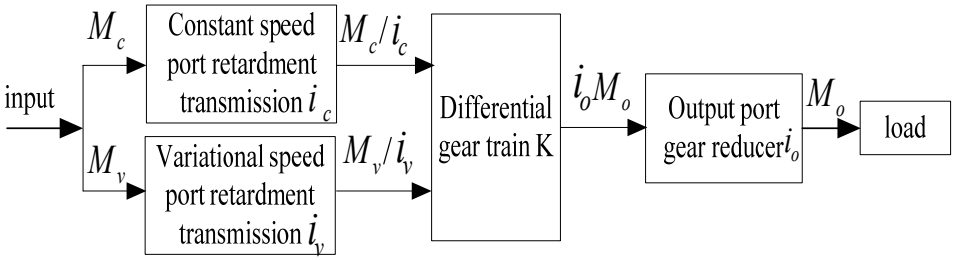

Figure 4. Hybrid-driven differential gear trains torque analysis

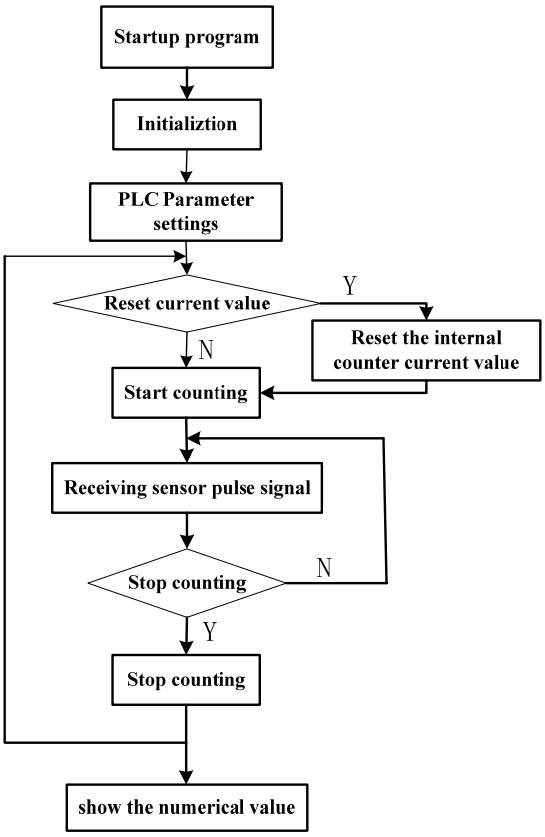

Figure 5. PLC program flow diagram

Modern Applied Science
www.ccsenet.org/journal.html
Vol. 3, No. 9
September 2009

The Model-Matching Error and Optimal Solution in Locally Convex Space

Lixin Ma
Department of Mathematics, Dezhou University, Dezhou 253023, China
E-mail: malixin6019@yahoo.com.cn

Abstract

The model-matching error and the optimal solution in the Hardy space are extended to the locally convex space, and the model-matching error and the optimal solution in the locally convex space are achieved. Thereby the ordinary H_∞-control theory is extended to with range in locally convex spaces through a form of a parameter vector. The algorithms of computing the infimal model-matching error and the infimal controller are presented.

Keywords: Locally convex space, Inner-outer function, Minimal realization, Infinal model- matching error

1. INTRODUCTION

Assume that R is the real field and R^n is the Cartesian product of n copies of R, here n is any positive integer, and that C is a complex plane.

To solve the problem for simplicity, we apply the $G(s)$ in the model matching problem to $G(s,\xi)$,where s in C, ξ in R^n,and $G(s,\xi)$ is in $C^\infty(R^n)$ (locally convex space) for each fixed s in C and in H_∞ for each fixed ξ in R^n. First, we extend several concepts.

Definition 1 The locally convex space VH_∞ consists of all complex-valued parameter functions $F(s,\xi)$ of a complex variable s and a parameter ξ which are analytic and bounded about s in $\mathrm{Re}\, s > 0$ (for each fixed ξ in R^n). Similarly, we define the VH_∞-norm of $F(s,\xi)$ is

$$|||\, F\, |||_\infty = \sum_{k=1}^{\infty} \frac{g_k}{2^k (1+g_k)},$$

where $g_k = \sup_{-k<\xi<k} \left\| F(\bullet,\xi) \right\|_\infty$

Definition 2 The subset of VH_∞ consists of all real-rational functions of s and ξ,will be denoted by VRH_∞.

Definition 3 Let α denote the infimal model-matching error

$$\alpha = \inf\{|||\, T_1 - T_2 Q T_3\, |||_\infty : Q \in VRH_\infty\}. \tag{1}$$

A matrix Q in VRH_∞ satisfying $\alpha = |||\, T_1 - T_2 Q T_3\, |||_\infty$ will be called optimal,where α is a model-matching error.

When $T_i(s,\xi)$ are scalar-valued,then there is no need for both $T_2(s,\xi)$ and $T_3(s,\xi)$.So we may as well suppose $T_3(s,\xi) = 1$.It is also assumed that $T_2^{-1}(s,\xi) \in VRH_\infty$ to avoid the trivial instance of the problem.

Returning to the model-matching problem, bring in an inner-outer factorization of

$T_2(s,\xi) : T_2(s,\xi) = T_{2i}(s,\xi) T_{2o}(s,\xi)$,

we have

$$|||\, T_1 - T_2 Q\, |||_\infty = |||\, R - X\, |||_\infty. \tag{2}$$

We conclude that

$$\alpha = \inf\{|||\, R - X \,|||_\infty : X \in VRH_\infty\} = dist(R, VRH_\infty). \tag{3}$$

Definition 4 The VL_p space, $1 \le p < \infty$,will be viewed as p th power integrable functions about s and ξ.When $p = \infty$, VL_∞ is the space of essentially bounded functions(for any fixed ξ in R^n).

Definition 5 The VRL_p space, VRL_p ,will be viewed as a subset of VL_p ,which consists of all real-rational functions of s and ξ.

Definition 6

(i) Let $F(s,\xi) \in VL_\infty$ and $g(s,\xi) \in VL_2$ .Then the operator

$$\Lambda_{F(s,\xi)} : \Lambda_{F(s,\xi)} g(s,\xi) = F(s,\xi) g(s,\xi)$$

is called the Laurent operator.

(ii) A related operator is $\Lambda_{F(s,\xi)} \mid VH_2$,the restriction of

$\Lambda_{F(s,\xi)}$ to VH_2 ,which maps VH_2 to VL_2 ,where $F(s,\xi) \in VL_\infty$.

(iii) For t $F(s,\xi) \in VL_\infty$,the Hankel operator with symbol $F(s,\xi)$,denoted by $\Gamma_{F(s,\xi)}$, maps VH_2 to ${VH_2}^\perp$ and is defined as

$$\Gamma_{F(s,\xi)} = \Pi_1 \Lambda_{F(s,\xi)} \mid VH_2 ,$$

where $VL_2 = VH_2 \oplus {VH_2}^\perp$,and Π_1 is the projection from VL_2 onto ${VH_2}^\perp$.

Definition 7 We call $F(s,\xi)$ to be strong proper if $F(s,\xi) \in VRH_\infty$ and $\sup_{\xi \in R^n} |F(\bullet,\xi| < \infty$,strictly strong proper if $F(\infty,\xi) \equiv 0$.

Definition 8 We call $F(s,\xi)$ to be stable if $F(s,\xi) \in VRH_\infty$ and $F(s,\xi)$ has no poles in the closed right half-plane $\mathrm{Re}\, s \ge 0$ (for each fixed ξ in R^n).

If $F(s,\xi)$ is real-rational about s in $\mathrm{Re}\, s > 0$, then $F(s,\xi) \in VRH_\infty$ if and only if F is strong proper and stable (for each fixed ξ in R^n). Similarly, we define

$$G(s,\xi) = \begin{bmatrix} T_1(s,\xi) & T_2(s,\xi) \\ T_2(s,\xi & 0 \end{bmatrix}, K(s,\xi) = -Q(s,\xi) ,$$

then the model-matching problem is

$|||\, T_1 - T_2 Q T_3 \,||| = \min imum$,

where $T_i (i = 1,2,3) \in VRH_\infty$ .The constraint that K stabilizes G is equivalent to that $Q \in VRH_\infty$.

We shall give in the form of parameter valued case the algorithms of computing the model-matching error α and the optimal controller Q .

2. THE MINIMAL REALIZATION

Definition 9 The linear time invarient system S_1 defined by

$$\dot{x}(t,\xi) = A(\xi)x(t,\xi) + B(\xi)u(t,\xi) \tag{4}$$

$$y(t,\xi) = C(\xi)x(t,\xi) \tag{5}$$

Where $A(\xi)$ is $n \times n$, $B(\xi)$ is $n \times m$,and $C(\xi)$ is $r \times n$ constant matrix depending on ξ ,is said to be completely controllable if the $n \times mn$ controllability matrix

$$U(\xi) = [B(\xi), A(\xi)B(\xi), ..., A^{n-1}(\xi)B(\xi)] \tag{6}$$

has rank n ,denoted by $(A(\xi), B(\xi))$.

Definition 10 The system S_1 described by (1) and (2) is completely observable if the observability matrix

$$V^T(\xi) = [C(\xi), C(\xi)A(\xi), ..., C(\xi)A^{n-1}(\xi)]^T \tag{7}$$

has rank n ,denoted by $(A(\xi), C(\xi))$.

Definition 11 Given an $r \times m$ matrix $G(s,\xi)$ whose elements are rational functions of s ,we wish to find matrices $A(\xi), B(\xi)$ and $C(\xi)$ depending on ξ ,having dimensions $n \times n, n \times m$ and $r \times n$ respectively, such that

$$G(s,\xi) = C(\xi)(sI_n - A(\xi))^{-1}B(\xi) \quad (5) \tag{8}$$

where I_n is the unit matrix of order n .

$[A(\xi), B(\xi), C(\xi), 0]$ is termed a realization of $G(s,\xi)$ of order n ,and is not, of course, unique. All such the above realizations will include matrices $G(s,\xi)$ having the least dimensions-be called the minimal realizations.

Definition 12 The Laplace transform of parameter-valued function $f(s,\xi)$ is defined by

$$F(s,\xi) = \int_0^\infty f(t,\xi)e^{-st}dt = Lf(t,\xi) \tag{9}$$

and the inverse Laplace transform of $F(s,\xi)$ is

$$f(t,\xi) = \int_{\sigma-j\infty}^{\sigma+j\infty} F(s,\xi)e^{st}ds = L^{-1}F(s,\xi) \tag{10}$$

we take the Laplace transform of (9) with zero initial conditions, we have

$$s\hat{x}(s,\xi) = A(\xi)\hat{x}(s,\xi) + B(\xi)\hat{u}(s,\xi)$$

and after rearrangement

$$\hat{x}(s,\xi) = (sI_n - A(\xi))^{-1}B(\xi)\hat{u}(s,\xi) \tag{11}$$

Since from (10) the Laplace transform of the output is

$$\hat{y}(s,\xi) = C(\xi)\hat{x}(s,\xi) \tag{12}$$

clearly

$$\hat{y}(s,\xi) = C(\xi)(sI_n - A(\xi))^{-1}B(\xi)\hat{u}(s,\xi) = G(s,\xi)\hat{u}(s,\xi) \tag{13}$$

where the $r \times m$ matrix

$$G(s,\xi) = C(\xi)(sI_n - A(\xi))^{-1}B(\xi) \tag{14}$$

Suppose $R(S,\xi) = [r_{ij}(s,\xi)]$ is an $p \times m$ strictly proper rationalfraction matrix of s (for any fixed ξ in R^n).

Theorem 1 A realization $[A(\xi), B(\xi), C(\xi), 0]$ of a given transfer matrix $G(s,\xi)$ is minimal if $(A(\xi), B(\xi))$ is *c.c.* and $(A(\xi), C(\xi))$ *c.o.*

Proof Let $U(\xi)$ and $V(\xi)$ be the controllability and observability matrices in (5) and (6) respectively. We wish to show that if these both have rank n then $R(s,\xi)$ has

least order n .

Suppose that there exists a realization $\{\overline{A}(\xi), \overline{B}(\xi), \overline{C}(\xi)\}$

of $R(s,\xi)$,with $\overline{A}(\xi)$ having order n_1 . Since

$$C(\xi)(sI_m - A(\xi))^{-1}B(\xi) = \overline{C}(\xi)(sI_m - \overline{A}(\xi))^{-1}\overline{B}(\xi),$$

It follows that

$$C(\xi)e^{A(\xi)t}B(\xi) = \overline{C}(\xi)e^{\overline{A}(\xi)t}\overline{B}(\xi),$$

Which implies, using the series

$(e^{A(\xi)t} = I + tA(\xi) + \frac{t^2}{2}A^2(\xi) + ...),$ that

$$C(\xi)A^i(\xi)B(\xi) = \overline{C}(\xi)\overline{A}^i(\xi)\overline{B}(\xi) \qquad i = 0,1,2,...$$

Consider the product

$$V(\xi)U(\xi)=\begin{bmatrix}C(\xi)\\C(\xi)A(\xi)\\.\\.\\C(\xi)A^{n-1}(\xi)\end{bmatrix}\left[B(\xi),A(\xi)B(\xi),...,A^{n-1}(\xi)B(\xi)\right]$$

$$=\begin{bmatrix}C(\xi)B(\xi) & C(\xi)A^{n-1}(\xi)B(\xi)\\.&.\\C(\xi)A^{n-1}(\xi) & C(\xi)A^{2n-2}(\xi)B(\xi)\end{bmatrix}$$

$$=\left[\overline{B}(\xi),\overline{A}(\xi)\overline{B}(\xi),...,\overline{A}^{n-1}(\xi)\overline{B}(\xi)\right]=V_1(\xi)U_1(\xi).$$

By assumping, $V(\xi)$ and $U(\xi)$ both have rank n, so the matrix $V_1(\xi)U_1(\xi)$ also have rank n. However, the dimension of $V_1(\xi)$ and $U_1(\xi)$ are respectively $r_1 n\times n_1$ and $n_1\times m_1 n$, where r_1 and m_1 are positive integers, so that the rank of ix $V_1(\xi)U_1(\xi)$ can not be greater than n_1. That is, $n<n_1$, so there can be no realization of $G(s,\xi)$ having order less than n.

3. INFIMAL MODEL-MATCHING ERROR

The Lyapunov equations are

$$A(\xi)L_c(\xi)+L_o(\xi)A^{\mathrm{T}}(\xi)=B(\xi)B^{\mathrm{T}}(\xi) \tag{15}$$

$$A^{\mathrm{T}}(\xi)L_o(\xi)+L_o(\xi)A(\xi)=C^{\mathrm{T}}(\xi)C(\xi) \tag{16}$$

Define the two controllability and observability gramians:

$$L_c(\xi)=\int_0^\infty e^{-A(\xi)t}B(\xi)B^{\mathrm{T}}(\xi)e^{-A^{\mathrm{T}}(\xi)t}dt,$$

$$L_o(\xi)=\int_0^\infty e^{-A^{\mathrm{T}}(\xi)t}C^{\mathrm{T}}(\xi)C(\xi)e^{-A(\xi)t}dt.$$

Theorem 2 $L_c(\xi)$ and $L_o(\xi)$ are the unique solutions of (12) and (13) respectively.

Proof Using the definition we have $A(\xi)L_c(\xi)+L_c(\xi)A^{\mathrm{T}}(\xi)$

$$=\int_0^\infty (A(\xi)e^{-A(\xi)t}B(\xi)B^{\mathrm{T}}(\xi)e^{-A^{\mathrm{T}}(\xi)t}+ e^{-A(\xi)t}B(\xi)B^{\mathrm{T}}(\xi)e^{-A^{\mathrm{T}}(\xi)}A^{\mathrm{T}}(\xi))dt = B(\xi)B^{\mathrm{T}}(\xi)-\lim_{t\leftarrow\infty}(e^{-A(\xi)t}B(\xi)B^{\mathrm{T}}(\xi)e^{-A^{\mathrm{T}}(\xi)t}).$$

Since $A(\xi)$ is instable,

$$\lim_{t\to\infty}(e^{-A(\xi)t}B(\xi)B^{\mathrm{T}}(\xi)e^{-A^{\mathrm{T}}(\xi)t})=0.$$

So $L_c(\xi)$ are the unique solutions of (12).From the discussion above, the uniqueness is obvious.

$L_o(\xi)$ are the unique solutions of (13) follows similarly.

Q.E.D.

Definition 13 Suppose the linear operator

$$T: X\to Y,$$

it's the unique operator

$$T^*: Y^*\to X^*,$$

Satisfying

$$(T^* y^*, x)=(y^*, Tx), x\in X^*, y\in T^*,$$

T^* is called the adjoint of T.

Define

$$f(s,\xi)=[A(\xi),\omega(\xi),C(\xi),0],$$
$$g(s,\xi)=[-A^{\mathrm{T}}(\xi),\lambda^{-1}(\xi)L_0(\xi)\omega(\xi),B^{\mathrm{T}}(\xi),0], \tag{17}$$

and

$$X(s,\xi)=R(s,\xi)-\lambda(\xi)f(s,\xi)/g(s,\xi). \tag{18}$$

So

$$f(s,\xi)=C(\xi)(sI-A(\xi))^{-1}\omega(\xi)\in VRH_2{}^{\perp},$$

and

$g(s,\xi)=B^{\mathrm{T}}(\xi)(sI+A^{\mathrm{T}}(\xi))^{-1}\lambda^{-1}(\xi)L_o(\xi)\omega(\xi)\in VRH_2$.

Theorem 3 [4] There exists a closest VRH_∞ -function $X(s,\xi)$ to a given VRL_∞ -function $R(s,\xi)$, and $|||R-X|||=\|\Gamma_R\|$.

Factor $R(s,\xi)$ as

$$R(s,\xi)=R_1(s,\xi)+R_2(s,\xi)$$

With $R_2(s,\xi)$ strictly proper and analytic in $\mathrm{Re}\,s<0$ and $R_2(s,\xi)$ in VRH_∞. Then $R_1(s,\xi)$ has a minimal state-space realization

$$R_1(s,\xi)=[A(\xi),B(\xi),C(\xi),0]$$

Define

$$L_c(\xi)=\lambda(\xi)\omega(\xi) \tag{19}$$

$$L_0(\xi)=\lambda(\xi)\nu(\xi) \tag{20}$$

Lemma 4 The function $f(s,\xi)$ and $g(s,\xi)$ satisfying equations

$$\Gamma_{R(s,\xi)}g(s,\xi)=\lambda(\xi)f(s,\xi) \tag{21}$$

$$\Gamma^{*}{}_{R(s,\xi)}f(s,\xi)=\lambda(\xi)g(s,\xi) \tag{22}$$

Proof to prove (21) start with (15). Add and subtract $sL_c(\xi)$ on the left-hand side to get

$$-(sI-A(\xi))L_c(\xi)+L_c(\xi)(sI+A^{\mathrm{T}}(\xi))=B^{\mathrm{T}}(\xi)B(\xi)$$

Now pre-multiply by $C(\xi)(sI-A(\xi))^{-1}$ and pre--multiply by $(sI+A^{\mathrm{T}}(\xi))^{-1}\nu(\xi)$ to get

$$\begin{aligned}&-C(\xi)L_c(\xi)(sI+A^{\mathrm{T}}(\xi))\nu(\xi)+C(\xi)(sI-A(\xi))^{-1}L_c(\xi)\nu(\xi)\\&=C(\xi)(sI-A(\xi))^{-1}B(\xi)B^{\mathrm{T}}(\xi)(sI+A^{\mathrm{T}}(\xi))^{-1}\nu(\xi)\end{aligned} \tag{23}$$

The first function on the left-hand side belong to VH_2 ; from (17) and (19) the second function equals $\lambda(\xi)f(s,\xi)$;and from (18) and (19) the function on the right-hand side equals $R_1(s,\xi)g(s,\xi)$. Project both side of (23) onto $VRH_2{}^{\mathrm{T}}$ to get

$$\lambda(\xi)f(s,\xi)=\Pi_1R_1(s,\xi)g(s,\xi)=\Gamma_{R_1(s,\xi)}g(s,\xi)\,.$$

But $\Gamma_{R(s,\xi)}=\Gamma_{R_1(s,\xi)}$; hence (21) dolds.

Equation (22) is proved similarly starting with (16). Q.E.D.

From Lemma 4, we can conceive

Corollary 5 $\left\|\Gamma_{R(s,\xi)}\right\|=\lambda(\xi)$

Theorem 6 The infimum model-matching error α equals $\lambda(\xi)$, the unique optimal X equals

$$R(s,\xi)-\lambda(\xi)\frac{f(s,\xi)}{g(s,\xi)}\,.$$

Proof from Theorem 3 there exists a function $X(s,\xi)$ in VH_∞ such that

$$\left\| R - X \right\|_{\infty} = \left\| \Gamma_{R(s,\xi)} \right\| \tag{24}$$

It is claimed that every $X(s,\xi)$ in VH_{∞} satisfying (24) also satisfies

$$R(s,\xi) - X(s,\xi)g(s,\xi) = \Gamma_{R(s,\xi)}g(s,\xi) \tag{25}$$

But (25) has a unique solution, namely,

$$X(s,\xi) = R(s,\xi) - \lambda(\xi)\frac{f(s,\xi)}{g(s,\xi)}.$$

Thus (21) and Theorem 3 imply

$$\alpha(\xi) = \lambda(\xi).$$

Therefore

$$X(s,\xi) = R(s,\xi) - \alpha(\xi)\frac{f(s,\xi)}{g(s,\xi)}.$$

Set

$$\alpha(\xi) = \lambda(\xi), \qquad Q(s,\xi) = T_2^{-1}(s,\xi)X(s,\xi). \tag{26}$$

Since $T_{20}(s,\xi), T_{20}^{-1}(s,\xi) \in VRH_{\infty}$,(26) sets up a one-to-one correspondence between functions $Q(s,\xi)$ in VRH_{∞} and functions $X(s,\xi)$ in VRH_{∞}. An optimal $X(s,\xi)$ yields an optimal $Q(s,\xi)$ via (24)

For a single-input and single-output design in the form of parameter valued case, we have similar to ordinary computing method.

Example.

$$P(s,\xi) = \frac{(s-1)(s-2)}{(s+1)(s^2+s+1+\xi^2)} \in VRH_{\infty}, \omega_1 = 0.01,$$

$$\varepsilon = 0.1.$$

From the above method, we derive

$$K(s,\xi) = \frac{0.615(s+0.4)(s+1)(s^2+s+1+\xi^2)}{s^4+6.145s^3+12.54s^2+13.53s+0.0232}.$$

Note $K(s,\xi) \notin RH_{\infty}$, but $K(s,\xi) \in VRH_{\infty}$.

Step 1. $$-P(s,\xi) = \frac{N(s,\xi)}{M(s,\xi)},$$

$$N(s,\xi) = -P(s,\xi), M(s,\xi) = 1 = X(s,\xi), Y(s,\xi) = 0.$$

Step 2.

$$W(s,\xi) = \frac{s+1}{10s+1}.$$

Step 3. $$T_1(s,\xi) = \frac{(s+1)^k}{(10s+1)^k},$$

$$T_2(s,\xi) = -\frac{(s+1)^k(s-1)(s-2)}{(10s+1)^k(s+1)(s^2+s+1+\xi^2)},$$

$$V(s) = s+1.$$

Step 4. When $k=1$,

Step (1) $$T_{21}(s,\xi) = \frac{(s-1)(s-2)}{(s+1)(s+2)},$$

$$T_{20} = -\frac{(s+1)(s+2)}{(10s+1)(s^2+s+1+\xi^2)}.$$

Step (2) $$R(s,\xi)=\frac{(s+1)^2(s+2)}{(10s+1)(s^2+s+1+\xi^2)}$$

the minimal realization is

$$A=\begin{bmatrix}1 & 0\\ 0 & 2\end{bmatrix},\quad B=\begin{bmatrix}-\frac{12}{11}\\ \frac{12}{7}\end{bmatrix},\qquad C=\begin{bmatrix}1 & 1\end{bmatrix}.$$

Step (3) $$L_c=\begin{bmatrix}\frac{72}{121} & -\frac{48}{77}\\ -\frac{48}{77} & \frac{36}{49}\end{bmatrix},\qquad L_0=\begin{bmatrix}\frac{1}{2} & \frac{1}{3}\\ \frac{1}{3} & \frac{1}{4}\end{bmatrix}.$$

Step (4) $$L_cL_0=\begin{bmatrix}0.0898 & 0.0425\\ -0.0668 & -0.0853\end{bmatrix}.$$

Then

$$\alpha_1=0.2299>0.1.$$

When $k=2$,

Step (1) $$T_{21}(s,\xi)=\frac{(s-1)(s-2)}{(s+1)(s+2)},$$

$$T_{20}=-\frac{(s+1)(s+2)}{(10s+1)(s^2+s+1+\xi^2)}.$$

Step (2) $$R(s,\xi)=\frac{(s+1)^3(s+2)}{(10s+1)^2(s^2+s+1+\xi^2)}$$

the minimal realization is

$$A=\begin{bmatrix}1 & 0\\ 0 & 2\end{bmatrix},\qquad B=\begin{bmatrix}-\frac{24}{121}\\ \frac{12}{49}\end{bmatrix},\qquad C=\begin{bmatrix}1 & 1\end{bmatrix}.$$

Step (3) $$L_c=\begin{bmatrix}\frac{24.12}{121.121} & -\frac{8.12}{121.49}\\ -\frac{8.12}{121.49} & \frac{12.3}{49.49}\end{bmatrix},\qquad L_0=\begin{bmatrix}\frac{1}{2} & \frac{1}{3}\\ \frac{1}{3} & \frac{1}{4}\end{bmatrix}.$$

Step (4) $$L_cL_0=\begin{bmatrix}0.0044 & -0.0025\\ 0.0031 & -0.0017\end{bmatrix}.$$

Then

$$\alpha_1=0.05113<0.1,\qquad \omega=\begin{bmatrix}1\\ -0.7209\end{bmatrix}.$$

Step (5) $$f(s,)=\frac{0.2791s-1.2791}{(s-1)(s-2)}$$

$$g(s)=\lambda^{-1}\frac{-0.0141s-0.0657}{(s+1)(s+2)}$$

$$X(s)=6.15\frac{(s+1)(s+2)(s+0.4)}{(10s+1)^2(s+4.66)}.$$

Step(6) Set

$$\alpha = \lambda = 0.05113$$

$$Q(s,\xi) = -6.15\frac{(s+0.4)(s^2+s+1+\xi^2)}{(s+1)(s+4.66)}$$

Step 5. $$Q_\alpha(s,\xi) = -6.15\frac{(s+0.4)(s^2+s+1+\xi^2)}{(10s+1)(s+1)(s+4.66)},$$

$$K(s,\xi) = 0.615\frac{(s+0.4)(s+1)(s^2+s+1+\xi^2)}{s^4+6.145s^3+12.54s^2+13.53s+0.0232}.$$

References

Francis, B.A. (1987). A course in H_∞-Control Theory. Spring-Verlag, Berlin. Heidelberg. New York, 1987. 61-80.

Francis, B.A., & Doyle, J.C. (1987). Linear Control Theory with an H_∞-Optimality Criterion. *SIAM control and Optimization*, 1987. 25: 815-844.

Francis, B.A., & Zames, G. (1984). On H_∞-Optimal Sensitivity Theory for SISO Feedback System. *IEEE Trans. Auto Cont,* 1984. AC-29: 9-16.

Kerulen, B.V. (1993). H_∞-Control with Measurement-Feedback for Infimite-Dimensional Systems. *Journal Mathematical Systems*, Estimation and control, 1993.3: 373-411.

Modern Applied Science
www.ccsenet.org/journal.html
Vol. 3, No. 9
September 2009

Higher Education Tuition Standard Model Analysis

Dongping Wang
School of Economics, Tianjin Polytechnic University
Tianjin 300160, China
E-mail: hebeimt@sohu.com

Tao Ma
School of Economics, Tianjin Polytechnic University
Tianjin 300160, China
E-mail: hebeimt@sohu.com

Fund: The national educational science "Eleventh Five-Year Plan" object (NO.DGA080073)

Abstract

Reform of higher education tuition in China is an important aspect of the reform of higher education and a problem which is urgent need to solve from "elite education" to "public education". "pay tuition to study ", "who invests ,Who benefits " have become a society-wide consensus. This paper mainly examines the impact of the average education cost, school level, advantages of location and school categories on university tuition fees, we set up the planning model with the analytic hierarchy process and quantitative analysis method .we focus on a national key university in Beijing and an ordinary university in Hebei province to analysis their tuitions which selected from 606colleges and universities of china.

Keywords: Charge differently, Quantitative analysis, AHP, Higher Education

The reasonableness of higher education tuition fees has been widespread concerned and studied. The proportion of higher education student tuition fees that accounts for the education costs and the proportion of higher education tuition fees that accounts for the average annual income of the family should remain at what level can we guarantee the quality of universities teaching and not give a heavy burden to most family?

The determination of higher education tuition fees in higher education is based on a certain amount of information .there are many factors that affect the higher education fees ,such as average student training costs, the average annual household income, university type, the location of university and economic status, university level, the state funding, personal expected return ,etc. However those data are incomplete and those indicators are different, so we make a number of appropriate methods in this paper to collect and deal with these information. For example, when we deal with the data of average student training costs, we reform the range standardization method to quantify the data between 0.5 and 1.

Firstly, Data collection and extraction. We get those related data such as average student training costs, the state financial allocations, the average annual household income data from China Statistical Yearbook and China Educational Finance Statistical Yearbook. At the same time we search related websites and books to obtain information on university category, the location of school and economics. And we extract and collate data with Excel, LINGO, SPSS software.

Secondly, Making a model. We transform the problem about the higher education reasonable tuition fees into a problem to maximize the quality of education which is bound by the residents' ability to pay for tuition. Among them, there are many factors to affect the number of tuition fees, we should quantify these factors and make a non-dimensional analysis, using AHP to determine the weights of various factors, to ensure the highest number of tuition fees is not more than 15% of the average household income. We take the average of standardized values of all the higher education tuition fees as tuition standard, therefore to work out the tuition Fees of all the universities. Tuition fees for higher education

should be based on urban residents' and rural residents' affordability of households to pay, and to ensure their commitment to the tuition fees is equal.

Thirdly, the western region lags far behind the eastern region economically. For example, in 2007, Shanghai, Beijing, Zhejiang's urban residents' disposable income per capita reached 23623, 21989 and 20574 Yuan, but Gansu, Heilongjiang, Qinghai reached only 10012, 10245 and 10276 Yuan. The gap between them is so wide. Shanghai, Beijing, Tianjin's per capita net income of rural residents reached 10222, 9559 and 8752 Yuan, but Gansu, Guizhou, Yunnan's per capita net income of rural residents is only 2328,2374 and 2634 Yuan. Shanghai, Beijing, Tianjin's per capita net income of rural residents is 4 times as many as Gansu, Guizhou, Yunnan's. In order to better reflect the education fair, we set up model II to determine the different tuition fees according to the level of economic development of different regions.

1. Model assumptions and symbol system

1.1 Model assumptions

1) The proportion that higher education tuition fees account for the average cost of education and training is not more than 25%;

2) The proportion that higher education tuition fees account for the overall household income should be maintained within 15%;

3) In this paper, the model only researches the undergraduate course school that arranged before 606 in "Evaluation of the 2008 Chinese University Study";

4) Different charge in higher education, namely, urban and rural college students in accordance with its proportion of household income to pay the tuition fees, insisting the principle of fairness in education;

5) The model is improved that different charge in higher education is double different fees, that is urban and rural college students pay the tuition fees in accordance with its proportion of household income, and charge different tuition fees in different provinces, to insist the principle of fairness in education;

6) The average population in urban family is 3, and the average rural family is 4.

1.2 Symbol system

BK: National Financial allocations;

YQ: the expected return of individual students;

R: the proportion that urban families accounted for rural families;

a: the proportion that higher education tuition fees accounted for the average of every student's training costs;

b: the proportion that higher education tuition fees accounted for the family income;

AC: the average training costs of national higher education students;

CR: the rural per capita income;

UR: the urban per capita income;

Fi: the standardized scoring value of No.i school's tuition;

Ei: the tuition that No.i school charge;

K: school category;

Fimax: the maximum value of all researched academy's standardized scoring value;

C: the average training costs of every student;

L: location advantages;

AF: the standardized scoring value of all academies'' tuition;

T: university level;

CAF: the corresponding tuition of AF, namely, the average tuition of students;

CC j: the tuition that the No. j province's rural college student paid;

UC j: the tuition that the No. j province's urban college student paid

2. Setting up model

2.1 Data collection and analysis

The standards of higher education depends primarily on the average training cost of students, university category,

location advantages, university level and the average household income. Therefore, to solve these problems, we should search the related data and conduct an in-depth analysis. The main data collection is as follows:

1) The average training cost of university students in all regions

Predicting the average training cost of university students in all regions in 2008, it affects actual value of the 2008 when the year is closer, therefore, followed by five years of data from the weight value for 0.1, 0.15, 0.2, 0.25, 0.3.We use software to predict the average training cost of university students in all regions in 2008.

Standardized the average training cost of university students in 2008: the improvement of range standardization.

According to the initial model, the greater the average training cost is, the higher charging standards are. The improvement of range standardization is as follows:

$X_{\max} = 32715(Beijing), X_{\min} = 8171(Guizhou\ \mathrm{Pr}ovince)$

Year / Region	2003	2004	2005	2006	2007	Prediction of 2008	standardization value of 2008
Beijing	32104	30823	30634	33592	34151	32715	1.00
Hebei	11574	11093	10612	10239	10152	10452	0.55

Data source: Based on China Educational Finance Statistical Yearbook from 2004 to 2008.

2) The level of university

According to the undergraduate course school that arranged before 606 in "Evaluation of the 2008 Chinese University Study", we standardize the rank of the college. Because the comprehensive strength of the top 100 schools in the rank is basically in accordance with the linear relationship between the decline and relatively large gap, so the top 100 schools are divided into 10 groups. As for, the 101-300 schools' gap is a little smaller, so select the class width is 20 and also divided into 10 groups. The gap of the last 306 schools' comprehensive strength is small, in order to show the otherness, we divide them into 10 groups and select the class width generally is 30.

Ways to assign ranks to the universities of standardized treatment, standardization formula is:

$$\beta_i = \cos(\frac{\pi}{90} * x)$$

Considering the ranking, total score, science research, personnel training and comprehensive reputation of the 606 colleges and universities, which have a great impact for the level of running a school, averaging the standardization of the five factors for the comprehensive level of running a school, then receive the standardized value of the level of university. The data of a national key university in Beijing and an ordinary university in Hebei province are as follows:

Rank	University	total score	science research	personnel training	comprehensive reputation	Result
2	A national key university in Beijing	96.09	100.00	88.53	93.03	0.978
128	An ordinary university in Hebei province	3.02	1.56	3.06	12.52	0.603

3) School category

For the type of colleges, we mainly consider 985, 211, provincial priorities and the Provincial ordinary university. For these four categories of schools is assigned to the standardization, valuing the 985 institutions for 4, 211 engineering colleges' assignment for 3, valuing the provincial priorities for the 2, and Provincial ordinary university for the 1. Take into account in the evaluation of students at colleges and universities, institutions of higher learning category for its gently diminishing the effectiveness of first and subsequently decreasing faster. Its membership functions as follows:

$$\phi(x) = \begin{cases} 0, x \le 1 \\ \frac{3}{4} + \frac{1}{4} * \sin\frac{\pi}{4}(x-2), 1 < x \le 4 \\ 1, \quad x > 4 \end{cases}$$

This function can through the colleges and universities to standardize the type of treatment and the values in [0.5, 1] interval. School standardized values of the categories are as follows:

School category	985	211	Provincial key university	Provincial ordinary university
ϕ_i	1	0.97	0.75	0.57

4) Regional advantage

The regional advantage of colleges and universities main to consider the geographical location of the advantage and disadvantage of various provinces and cities, as well as the level of economic development (per capita GDP) factors. The regional advantage has both economic factors and geographical factors. Therefore, we consider the per capita GDP of various provinces and cities as studying the level of economic development indicators, provinces and cities to maintain a relatively constant level of per capita GDP basis in the [0.5, 1] interval on standardization.

$$\gamma = 0.5 + 0.5 * \frac{x - x_{\min}}{x_{\max} - x_{\min}}$$

Refer to traditional Chinese geographical classification of the various provinces and cities, the country is divided into nine areas: Beijing and Shanghai, Tianjin and Guangzhou, East China, Central China, North China, Northeast, Southwest, South China, Northwest. Various provinces and cities in the standardization of the specific geographical location in the following table:

	Standardization value	Province and city		Standardization value	Province and city
Beijing, Shanghai	1	Beijing, Shanghai	northeast	0.7	Heilongjiang, Jilin, Liaoning
Tianjin, Guangzhou	0.9	Tianjin Guangzhou	southwest	0.65	Chuan, Gui, Yun, Zang, Yu
East China	0.85	Su, Zhe, Lu, Min, Wan, Gan	south China	0.6	Qiong, Gui
North China	0.75	Jin, Meng, Ji	northwest	0.5	Shan, Gan, Ning, Xin, Qing

Because of the level of economic development for regional advantage is greater than the impact of geographical location, may wish to check the proportion of 6:4, the composite calculated advantage of the standardized values. The data of a national key university in Beijing, an ordinary university in Hebei province are as follows:

university	region	standardized values of location advantage	university	region	standardized values of location advantage
A national key university in Beijing	Beijing	0.959	An ordinary university in Hebei province	Hebei	0.664

2.2 Setting up Model

Generally speaking the higher education tuition fees should not exceed 15% of the total household income, in order to ensure the quality of teaching, the school should raise adequate funding for teaching.

2.2.1 Analysis of setting up model

1) firstly, we consider the objective function max Ei=Fi/AF*AC*ai,

namely, after solving Fi, we get the maximum of ai, the objective function is that max ai.

2) then considering the constraint conditions

①the bound of tuition fees accounted for the proportion of the training costs: a_i<=25%.

National provides that university tuition fees accounted for the proportion of the training costs in general should not exceed 25%,

② tuition fees accounted for the proportion of total household income constraint: b_i<=15%.

the family affordability of tuition fees generally accounted for total household income does not exceed 15%.

③various colleges and universities should not exceed the maximum charge capacity of the residents

$$\frac{CAF * F_{i\max}}{AF} \le \frac{CR*4+UR*3R}{R+1} * 0.15$$

,

Suggesting the planning model as follows:

$$\begin{cases} \max E_i = \dfrac{F_i}{AF} * AC * a, \\ a_i \le 25\% \\ b_i \le 15\% \\ \dfrac{CAF * F_{i\max}}{AF} \le \dfrac{CR*4+UR*3R}{R+1} * 0.15 \end{cases}$$

3. Model Solution

3.1 Solving method

In the target function, the standardized value of the tuition fees of colleges and universities (Fi) are unknown. The factors that affect Standardized value of tuition fees are the average training cost of university student C, university Type K, the advantage of location L and university level T. We can use the data of Annex 1and Annex 2 to determine standardized number of the tuition fees of colleges and universities Fi with analytical hierarchy process.

3.2 The determination of the standardized value of tuition fees

The raw data of the factors that affect composite scores are Di, In the front we have already standardized the average training cost of university student C, university Type K, the advantage of location L and university level T. Using AHP method that bases on the index level of analysis to determine each university's total score. we set up the goal hierarchy in order to obtain the score of each university , as shown in Figure 1, the top layer is the target layer, middle layer is a criterion, the bottom layer is the program layer.

.

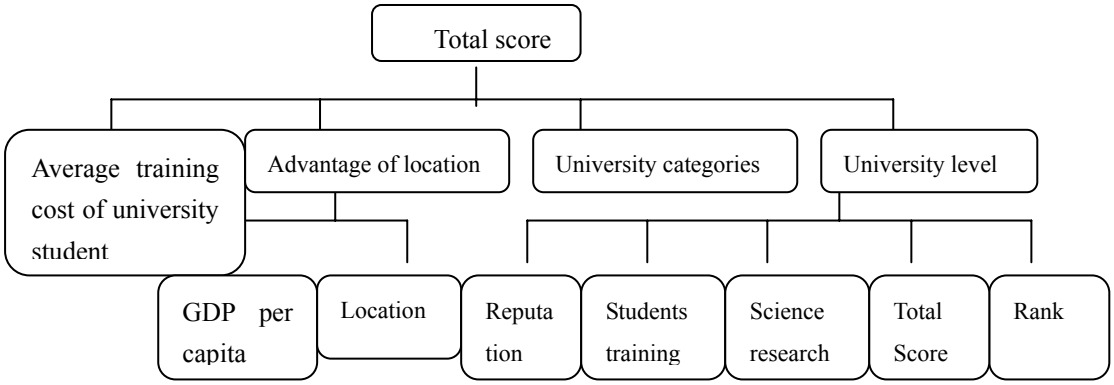

The indicators is better than the traditional 1-9 scale ,it overcomes the short-coming that its coherence is not equivalent with mind coherence and it is in accordance with the transfer guidelines, meanwhile the gap should not be too much between each factors. Checking the relative importance a = 1.618, the meaning of scaling index is as follows:

Scale aij	Scaling definition	Scale aij	Scaling definition
a0=1	Di is as important as Dj	a3=4.236	Di is important than Dj obviously
a1=1.618	Di is slightly important than Dj	a4=6.854	Di is very important compared to Dj
a2=2.618	Di is important than Dj	a5=11.09	Di is absolutely essential compared with Dj

Determining the matrix structure. Taking into account scoring, various factors on the impacts of tuition fees are not too big, so the weight of each factor should not be great different. In this paper, subjective judgments resulting matrix is as follows:

$$A=(a_{ij})_{4*4}=\begin{pmatrix}1 & a & a^2 & a^2\\ a^{-1} & 1 & a^2 & a^2\\ a^{-2} & a^{-2} & 1 & a\\ a^{-2} & a^{-2} & a^{-1} & 1\end{pmatrix}$$

We deal with the above-mentioned matrix with Mathematica program and make the consistency test. Obtaining the largest eigenvalue of matrix A is 4.015, consistency index CI = 0.0194 and consistency ratios CR = CI / RI = 0.022 <0.1, so CR = 0.022, their subjective judgments matrix pass the consistency test. Simultaneously we can get weight values of various factors are 0.405, 0.318, 0.155, 0.122.Further we can get the cost scores of university i:

$$F_i=\sum_{j=1}^{4} w_j\times q_{ij},(i=1,2,\ldots,606,\ j=1,2,3,4);$$

q_{ij} is stand for the standardization value of university I's factor J. The standardized values of National key universities in Beijing and an ordinary university in Hebei Province are as follows:

Rank	university	Tuition score	Rank	university	Tuition score
2	National key universities in Beijing	0.991	174	an ordinary university in Hebei Province	0.703

3.3 Model Solution

Fi is the standardized value 0f each university tuition fees we get from the above-mentioned solution. We substitute Fi into the above model and solve with LINGO 11.0 .We can get the data of National key universities in Beijing and an ordinary university in Hebei province based on the results:

Name of universities	The weighted average fees	The value of B	urban	rural
A national key university in Beijing	4406	0.150	6191	2479
An ordinary college in Hebei province	2819	0.096	3961	1586

4. Model improvement

When we solve the original model we find that the proportions of university tuition fees account for urban and rural household income are same. Meanwhile Peking University chare the highest tuition fees accounted for urban and rural household income, reaching 15%, just the maximum capacity to pay of the residents can bear. However, when we view urban residents' per capita disposable income and rural residents per capita net income in 2007, finding urban residents and rural residents' income in different regions of China are different significantly. Shanghai, Beijing, Tianjin's per capita net income of rural residents reached 10222, 9559 and 8752 Yuan, but Gansu, Guizhou, Yunnan's per capita net income of rural residents is only 2328,2374 and 2634 Yuan. Shanghai, Beijing, Tianjin's per capita net income of rural residents is 4 times as many as Gansu, Guizhou, Yunnan's.

Therefore the above model only consider the different fees between urban students and rural students from the whole country, the burden of education fee paid by different area varies largely. So we need to improve the above model. Here, this article introduces some parameter, Re_{ij} stands for the number of enrolling new students in ith university of jth province. b_i stands for the proportion of the education fee that university charge occupying the average annual income, R_i stands for the proportion between the urban family number of the jth province and rural family number, UR_j stands for the disposable income of urban residents from jth province, CR_j stands for the disposable income of rural residents from jth province, UC_j stands for the average annual education fee the urban residents from jth province should pay for, CC_j stands for the average annual education fee the rural residents from jth province should pay for.

Set up model as follows: $\sum_{j=1}^{31}\mathrm{Re}_{ij}\ y_i=\sum_{j=1}^{31}\left(\frac{R_j*UR_j*3*b_i+CR_j*4b_i}{R_j+1}\right)*\mathrm{Re}_{ij}$

$$\begin{cases} UC_j=UR_j*3b_i; \\ CC_j=CR_j*4b_i; \\ b_j\le 0.15; \end{cases}$$

We use this model to solve the tuition fees of urban students and rural students in all provinces, we get the tuition fees of a national key university in Beijing and an ordinary university in Hebei province in various provinces.

5. The results of improved model

We solve the improved model by the means of LINGO11.0 software, the results are as follows:

A national key university in Beijing				An ordinary college in Hebei province			
region	student intake	Urban tuition	Rural tuition	region	student intake	Urban tuition	Rural tuition
Beijing	295	10225	5927	Beijing	50	9664	5602
Hebei	50	5436	2662	Hebei	1000	5138	2516

6. The suggestion to relevant department

Higher education is important to high-standard person cultivation, innovation ability, the construction of harmonious society. But in present period of Chinese economic development, the unbalance of economic development and the unequal of residential income consist in our country to large extent. How to definite the higher education fee should be based on the payment of resident and the guarantee of fair education. In order to offer enough education funds and make large number of rural children t to attend the university. in other words, to make the proportion between higher education fee and common rural family income not too high ,we make few suggestions as follow:

(1) The university that rank former should charge relatively higher because the better universities` cultivation fee, the location advantage, the classification of school and the personal profit after graduation are relatively excellent. According to the principle that huge profit needs huge investment, acquiring high fee is reasonable. For example, Peking University which ranks first should charge higher than the other ordinary Universities.

(2) Each university should distinguish the rural children and the urban children to charge differently. Trough the model we can make preferential to rural children. But the payment of urban family is relatively strong. So we use the payment of urban family to make up for the shortage of rural family income, which involve the question that whether it reasonable or not. Because citizens enjoy some preferential condition in the unbalance of Chinese economic development, it can be accepted that difference consists in the higher education fee.

(3) Based on the different amounts shared by urban and country and the difference in each area, higher education fee should be fixed respectively according to different area. From the model, it can be found that the difference in area can be improved by the economic development (GDP per head levels) of district where students come from,, which makes students from different provinces pay for their fee based on the local actual economic condition.

(4)Through the model we build about 606 universities from the whole country, we can judge a school whether its fee are reasonable and offer the theoretical support to the reform of each school’s education fee.

References

2007 National Higher Education Admissions Guide aggregate admission schem. http://edu.qq.com/zt/2007/2007zsjz/index.htm**.** September 21st 2008

China Statistical Yearbook of the funding for education(2004-2008). Beijing:China Statistics Press. (in Chinese)

China Statistical Yearbook. (2008). Beijing: China Statistics Press. (in Chinese)

Li Z., Xiao H., et al. (2005). Fuzzy optimization method in the production of decision-making applications. *Journal of Southwest University for Nationalities*, 31(5),701-704. (in Chinese)

The people Republic of China National Bureau of Statistics(2008). Beijing:China Statistics Press. (in Chinese)

Xie J. and Liu C. (2000). Fuzzy Math Methods and Applications (2nd edition). Wuhan: Huazhong University of Science and Technology Press. (in Chinese)

Xie J.and Xue Y. (2005). Optimize Modeling and LINDO / LINGO software. Beijing: Tsinghua University Press. (in Chinese)

Xu Y. (2003). The index scale degrees in important research. *Journal of Textile Universities basic science*, 16(2) ,138-140. (in Chinese)

Zhao D., Cai Y., Feng Y., et al. (2008). 2008 Chinese University of evaluation reports. *Chinese Higher Education Evaluation*. the first phase. (in Chinese)

A journal archived in Library and Archives Canada
A journal indexed in CANADIANA (The National Bibliography)
A journal indexed in AMICUS
A journal indexed in Zentralblatt MATH
A journal included in the Chemical Abstracts database
A journal included in DOAJ (Directory of Open-Access Journal)
A journal included in Google Scholar
A journal included in LOCKSS
A journal included in PKP Open Archives Harvester
A journal listed in Journalseek
A journal listed in Ulrich's
A peer-reviewed journal in applied science research

Modern Applied Science

Monthly

Publisher Canadian Center of Science and Education
Address 4915 Bathurst St. Unit # 209-309, Toronto, ON. M2R 1X9
Telephone 1-416-208-4027
Fax 1-416-208-4028
E-mail mas@ccsenet.org
Website www.ccsenet.org
Printer William Printing Inc.
Price CAD.$ 20.00

ISSN 1913-1844